



**TALLINN UNIVERSITY OF TECHNOLOGY**  
SCHOOL OF ENGINEERING  
Department of Materials and Environmental Technology

# **ELECTROSPUN FILTER MATERIALS WITH ENHANCED PROTECTIVE PROPERTIES**

## **PARENDATUD KAITSEOMADUSTEGA ELEKTROKEDRATUD FILTERMATERJALID**

### MASTER'S THESIS

Student: Krista Laanemets

Student code: 204735KVEM

Supervisors: Dr. Natalja Savest, Senior Lecturer  
Dr. Anna-Liisa Kubo, Research Fellow  
(National Institute of Chemical Physics and  
Biophysics)  
Mihkel Viirsalu, Engineer

Tallinn 2022

**AUTHOR'S DECLARATION**

Hereby I declare, that I have written this thesis independently.  
No academic degree has been applied for based on this material. All works, major viewpoints and data of the other authors used in this thesis have been referenced.

"24" May 2022

Author: Krista Laanemets  
*/signature/*

Thesis is in accordance with terms and requirements

"24" May 2022

Supervisor: Natalja Savest  
*/signature/*

Accepted for defence

"....." .....20... .

Chairman of theses defence commission: .....  
*/name and signature/*

## **Non-exclusive Licence for Publication and Reproduction of Graduation Thesis<sup>1</sup>**

I, Krista Laanemets (date of birth: 24.01.1996) hereby

1. grant Tallinn University of Technology (TalTech) a non-exclusive licence for my thesis

Electrospun Filter Materials with Enhanced Protective Properties,  
(title of the graduation thesis)

supervised by Dr. Natalja Savest,  
(supervisor's name)

1.1 to be reproduced for the purposes of preservation and electronic publication, incl. to be entered in the digital collection of TalTech library until expiry of the term of copyright;

1.2 to be published via the web of TalTech, incl. to be entered in the digital collection of TalTech library until expiry of the term of copyright.

1.3 I am aware that the author also retains the rights specified in clause 1 of this licence.

2. I confirm that granting the non-exclusive licence does not infringe other persons' intellectual property rights, the rights arising from the Personal Data Protection Act or rights arising from other legislation.

---

<sup>1</sup> *Non-exclusive Licence for Publication and Reproduction of Graduation Thesis is not valid during the validity period of restriction on access, except the university's right to reproduce the thesis only for preservation purposes.*

\_\_\_\_\_ (signature)

"24" May 2022 (date)

**Department of Materials and Environmental Technology**

**THESIS TASK**

**Student:** Krista Laanemets, 204735KVEM (name, student code)

Study programme, KVEM12/20 - Technology of Wood, Plastic and Textiles

main speciality: 3 - technology of plastics and textiles

Supervisor(s): Dr. Natalja Savest, Senior Lecturer, +372 523 8393

Dr. Anna-Liisa Kubo, Research Fellow (National Institute of Chemical Physics and Biophysics), +372 512 1279

Mihkel Viirsalu, Engineer, mihkel.viirsalu@taltech.ee

**Thesis topic:**

(in English) Electrospun Filter Materials with Enhanced Protective Properties

(in Estonian) Parendatud kaitseomadustega elektrokedratud filtermaterjalid

**Thesis main objective:**

Successfully producing electrospun filter material with enhanced protective properties against viruses like SARS-CoV-2 by the means of electrospinning

**Thesis tasks and time schedule:**

No	Task description	Deadline
1.	Successfully producing electrospun materials with antimicrobial additives.	"19" December 2021
2.	Conducting tests and analysis on the electrospun materials.	"8" April 2022
3.	Analysing the results to determine the success of producing electrospun filter material with enhanced protective properties against viruses like SARS-CoV-2 by the means of electrospinning.	"20" May 2022

**Language:** English

**Deadline for submission of thesis:** "24" May 2022

**Student:** Krista Laanemets ..... ".....".....20.....a  
/signature/

**Supervisor:** Natalja Savest ..... ".....".....20.....a  
/signature/

**Head of study programme:** Jaan Kers ..... ".....".....20.....a  
/signature/

# CONTENTS

CONTENTS.....	5
PREFACE .....	6
List of abbreviations and symbols .....	7
1. INTRODUCTION .....	8
2. LITERATURE OVERVIEW .....	9
2.1 Electrospinning.....	9
2.1.1 Parameters Affecting Electrospinning .....	11
2.1.2 Materials Used in Electrospinning .....	13
2.1.3 Biobased filter materials.....	13
2.1.4 Advantages and Uniqueness of Electrospinning .....	14
2.2 Studying and Altering Electrospun Materials .....	16
2.2.1 Dispersion Analysis of Nanoparticle Additives .....	16
2.2.2 Deacetylation Of Cellulose Acetate for Improving Hydrophilicity .....	17
2.2.3 Fourier-Transform Infrared Spectroscopy .....	19
2.3 Air Filter Materials.....	20
2.3.1 Air filtration mechanisms.....	22
2.3.2 Electrospun filter materials in medicine field .....	24
3. EXPERIMENTAL PART .....	25
3.1 Materials and Methods.....	25
3.2 Results and discussion.....	31
3.2.1 Dispersion Analysis of Additives .....	31
3.2.2 Electrospinning of filter materials .....	31
3.2.3 Analysis of Hydrophilic Properties of the Electrospun Materials .....	36
3.2.4 FTIR analysis .....	38
3.2.5 Measurement of Metal Content of the Materials .....	42
3.2.6 Air Permeability of Electrospun Filter Materials .....	44
3.2.7 Effectiveness Of Aerosol Particles Filtration .....	46
3.2.8 Antibacterial Properties of Electrospun Filter Materials.....	47
3.2.9 Antiviral Properties of Electrospun Filter Materials.....	49
4. SUMMARY.....	51
5. KOKKUVÖTE .....	53
LIST OF REFERENCES .....	55

## PREFACE

The thesis topic was initiated by Dr. Anna-Liisa Kubo of National Institute of Chemical Physics and Biophysics and the majority of thesis work was done at Tallinn University of Technology, with the help of Senior Lecturer Dr. Natalja Savest and engineer Mihkel Viirsalu of the Laboratory of Polymers and Textile Technology.

Within the project, of which the thesis was a part of, the following people were of vital importance in research capacities in their respective fields, helping contribute to this thesis in data collecting capacities - Anna-Liisa Kubo, Research Fellow of Laboratory of Environmental Toxicology at National Institute of Chemical Physics and Biophysics, Kai Rausalu, Research Fellow of Institute of Technology at University of Tartu, Eva Zusinaite, Associate Professor of Virology at the Institute of Technology at University of Tartu, Grigory Vassiliev, Laboratory of Environmental Toxicology PhD student at the National Institute of Chemical Physics and Biophysics, Andres Krumme, Head of Laboratory at the Laboratory of Polymers and Textile Technology in Tallinn University of Technology, Andres Merits, the Professor of Applied Virology of Institute of Technology at University of Tartu, Olesja Bondarenko, Senior Researcher of Laboratory of Environmental Toxicology at National Institute of Chemical Physics and Biophysics. The source of funding for the project was COVSG16 "Novel nanoparticle-based filter materials and face masks for SARS-CoV-2 inactivation (1.10.2020–31.12.2021)", Olesja Bondarenko, National Institute of Chemical Physics and Biophysics. I would like to extend my deep gratitude to all those mentioned, especially Dr. Natalja Savest.

Master's thesis "Electrospun Filter Materials with Enhanced Protective Properties" succeeded in its aim to produce electrospun filter material with improved protective properties against viruses like SARS-CoV-2 by the means of electrospinning. Out of the three electrospun filter materials which had excellent test results, electrospun material produced from the solution of CA + **CuSO<sub>4</sub>** in Acetone-DMAc (2:1) showed the most promising results to be used as electrospun filter material with enhanced protective properties.

Keywords: Electrospinning, filter material, antimicrobial properties, nanoparticles, master's thesis

## List of abbreviations and symbols

Ag - silver

CA - cellulose acetate

Cu - copper

CuI - copper (I) iodide

CuO - copper oxide

$\text{Cu}_2(\text{OH})_2\text{CO}_3$  - basic copper carbonate

$\text{Cu}(\text{OH})_2$  - copper (II) hydroxide

$\text{CuSO}_4$  - copper sulphate

DLS - Dynamic Light Scattering

DMAc - dimethylacetamide

E. coli - Escherichia coli

EtOH - ethanol alcohol

MNPs - metallic nanoparticles

MRSA - methicillin-resistant Staphylococcus aureus

NaOH - sodium hydroxide

NP - nanoparticle

S. aureus - Staphylococcus aureus

SARS-CoV-2 - severe acute respiratory syndrome coronavirus 2

SEM - Scanning Electron Microscopy

TEM - Transmission Electron Microscopy

VOC - Volatile Organic Compounds

# 1. INTRODUCTION

Viruses like severe acute respiratory syndrome coronavirus 2 (SARS-CoV-2) have recently become a serious concern on a global level. It has been noted that such viruses are transmissible by air, the spread of these viruses is also directly linked to air pollution, which in itself is a great challenge of this century [1]. RNA viruses like SARS-CoV-2 are known to mutate into new variants, which are proving to be unpredictable in terms of resistance to vaccines, rate of spread and severity [2]–[4], thus using masks is critical for preventing the spread of SARS-CoV-2 [2], [5]. Electrospinning method has been studied as a potential method to produce nanofibrous filter materials [6]–[11], as nanofibers have shown exceptional results in removing viruses, airborne nanoparticles, bacteria and volatile organic compounds (VOC) from air stream [6], [12]. Various electrospinning solution additives can be used to create nanofiber materials with enhanced protective properties, such as transition metals copper, silver, copper oxides and other copper compounds. These additives are known for their antimicrobial properties and thus could enhance the protective properties of electrospun filter material [13].

The main problem to be solved is to create a method of producing electrospun filter materials with enhanced protective properties which are effective against serious respiratory viruses like SARS-CoV-2.

The aim and objective of this thesis is to successfully produce electrospun filter material with antiviral properties against viruses like SARS-CoV-2 by the means of electrospinning. The novelty of this thesis is based on using antimicrobial nanoparticle and metal compound additives in electrospinning solution to create nanofibrous filter materials with enhanced protective properties.

Within this thesis, a thorough overview of the electrospinning method is given, including parameters affecting the electrospinning process, advantages and uniqueness of the electrospinning method, materials used for electrospinning, including biobased filter materials. The topics of filter materials and viruses is discussed. Then an overview of all the materials, including the materials used to produce the electrospinning polymer solution and nanomaterials added to increase protective properties of the electrospun material is given. The methods and experimental part are discussed in detail, including polymer solution preparation process, ultrasound method, dispersion analysis of additives, scanning electron microscopy, thickness and air permeability measurements of electrospun materials, aerosol filtration efficiency test, contact angle measurement, deacetylation method, Fourier-Transform Infrared Spectroscopy, quantification of metal content, microbiological and antiviral tests. Finally, all test results are analysed before drawing the final conclusions.



## **2. LITERATURE OVERVIEW**

### **2.1 Electrospinning**

Electrospinning was patented in 1934 and is currently considered a very popular method for producing fibers with very small diameters. The scale of electrospun fiber diameters can range from micrometres ( $\mu\text{m}$ ) to nanometres (nm) [14], [15]. Electrospinning method is preferred over other methods of nanostructure production, because it can be used to produce nanofibers with exceptionally high specific surface area [16] and the overall structure of the process is simple. Improvements in the electrospinning process has helped make notable advancements in the fields of bioengineering, energetics, environmental protection and medicine.

In addition to the classic nanofiber electrospinning process, there are alternative nanostructure electrospinning processes as well, for example wet, molten, emulsion, and coaxial electrospinning [14], [15], [17]. In the case of wet electrospinning, the usually solid collector is replaced with a tub filled with collector-liquid. This serves the purpose of achieving fibers with fluffy structures [14]. Molten electrospinning does not use the toxic solvents that are characteristic to classic electrospinning [15], instead difficult to dissolve polymers [17] are deposited to the collector in an oriented fashion [14]. Molten electrospinning is considered an environmentally friendly option, as it does not require the use of solvents [14]. Emulsion electrospinning creates two layered nanofibers, which have a core and surrounding layer that are made from different polymer solutions [15]. Coaxial electrospinning uses coaxial capillaries to spin multiple polymer solutions [17].

The equipment used in a typical electrospinning process (Figure 2.1) consists of a syringe filled with electrospinning solution, that is connected to a power supply and fixed to a needle pump, as well as a DC motor that is connected to the grounded spinning collector [14].

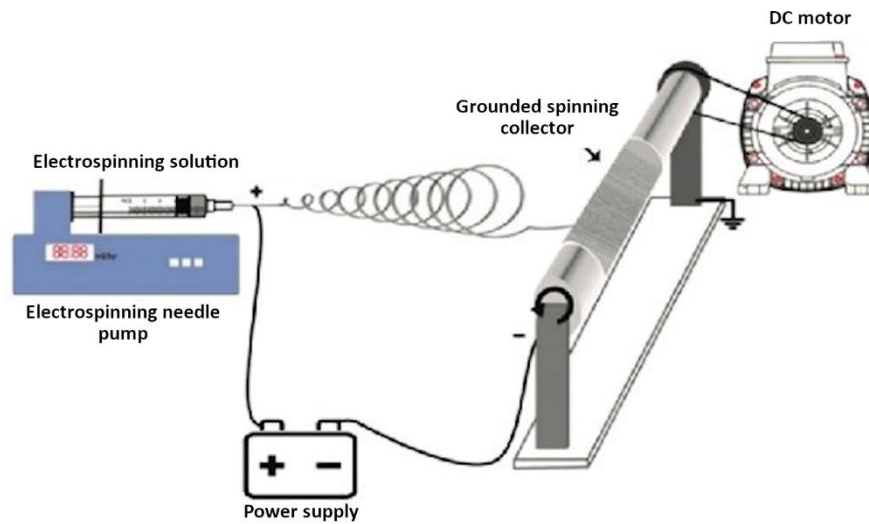


Figure 2.1 Set-up of electrospinning process [14]

Electrospinning process uses high voltage to create electrostatic forces in the viscose electrospinning polymer solution, which in turn helps create a conical droplet to the tip of the needle. This conical drop is called Taylor's cone (Figure 2.2), which ensures an effective electrospinning process [17].

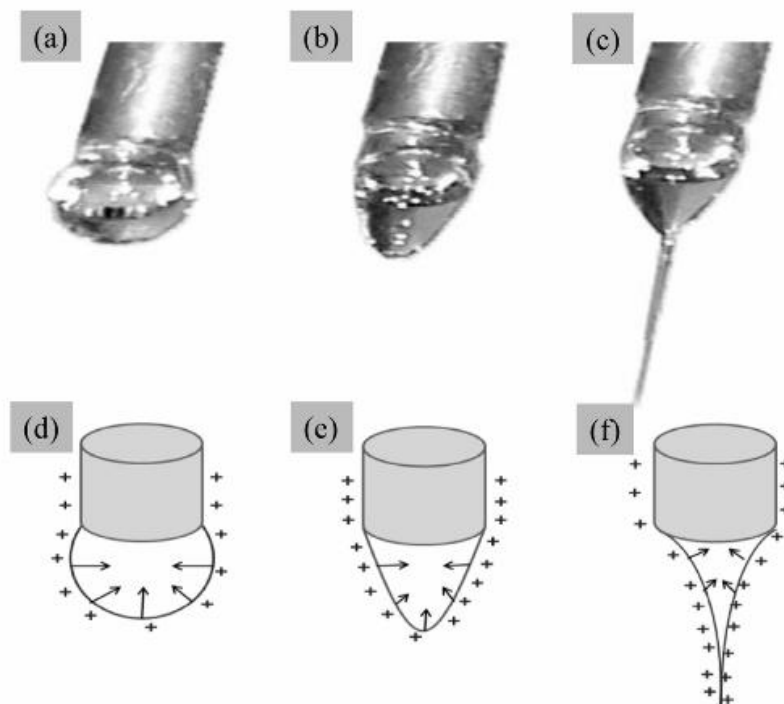


Figure 2.2 Creation of Taylor's cone [18]

After Taylor's cone has been created, the electrostatic forces exceed the surface tension of the drop [15] and the polymer solutions creates a jet and moves onto the spinning

grounded collector. Due to the forces subjected to this jet, before reaching the collector it acts in an unstable fashion (vibrates and stretches into a thinner jet) [17]. If the polymer concentration in the solution is too low, there is a chance that the jet will break down into droplets. If the concentration is sufficiently high, a uniform and constant jet is formed. As the solvent evaporates, the fiber diameter decreases, creating a solid and continuous fiber. The diameter of electrospun fibers can range from microscale to nanoscale [18].

In most cases, electrospun fibers land on the collector in a disorderly fashion, creating a non-woven nanofiber material. To achieve oriented nanofiber material, controlled fiber deposition methods are used, which are mostly based on a combination of mechanical rotation and electric field manipulation [15], [17].

Electrospun nanofibers may have a smooth or porous surface, a hollow core, or a side-by-side structure. Due to their diverse set of properties, electrospun nanofibers are being used in the fields of energetics, sensors, filtration systems and medicine [18].

### **2.1.1 Parameters Affecting Electrospinning**

Both the electrospinning process and the properties of the fibers are affected by many parameters, mainly the speed of pumping the solution [19], solution viscosity, solution conductivity, the distance between the tip of the needle and the collector, temperature, humidity and the applied voltage [15]. These parameters can be categorized as process parameters and environmental parameters.

#### **Process parameters**

The distance between the tip of the needle and the collector affects the properties of the fiber, as the precipitation time and the rate of evaporation of the solution depend directly on the distance between the needle and the collector. To achieve a uniform fiber, an optimal distance should be determined [17]. Although a few instances have been noted where the distance has not affected the morphology of the fiber [18], increasing the distance is still associated with decreased diameters of the fibers, whereas shorter distance is associated with increased fiber diameters. Matabola *et al* has found, that 28 wt% polyvinylidene fluoride (PVDF) solution electrospun with 12 kV voltage created 397 nm diameter fibers when 15 cm distance was used, and fibers with an average of 314 nm diameter were achieved when 16 cm distance was used [19].

When the applied voltage is above the critical level, uneven morphology of the fiber surface has been noted (bead formation) and fiber diameter is increased. Deitze *et al* found, that electrospinning of a solution of polyethylene oxide (PEO) and water (H<sub>2</sub>O) at 5.5 kV applied voltage created nanofibers with defect free morphology. However, when 9 kV voltage was applied, high bead concentration was noted on the surface of the fibers. It was found, that for the PEO/H<sub>2</sub>O system, critical level of voltage is 7 kV. Exceeding that voltage level caused electrospun fibers to have an uneven morphology [15]. Increasing the voltage causes the Taylor's cone size to decrease [17], and in some rare cases retreat back inside the needle tip [18]. However, using a voltage that is too low, will not allow for the charged jets of polymer solution to be ejected from the Taylor's cone, thus no electrospinning will occur [20].

Pumping speeds above the critical limit also affect the morphology of the fibers, causing the formation of beads. The reason behind this phenomenon is the insufficient drying of the fiber, as it moves between the needle tip and collector. Exceeding the critical limit of pumping speed also causes larger fiber diameters. As a rule of thumb, the lowest possible pumping speed is preferred, as it ensures an even creation of Taylor's cone [19].

### **Environmental parameters**

Fiber morphology and diameter are also affected by various environmental parameters, such as temperature and humidity. Humidity affects the rate at which the fiber hardens and dries, but the chemical properties of the polymer also play an important role. An increase in humidity reduces the diameter of the nanofiber, for example, when the humidity increases by 56%, the diameter of the polyvinyl alcohol (PVA) fiber decreases by 76%. The decrease in humidity causes the diameter of the electrospun nanofibers to increase. At low humidity levels, the solvent evaporates faster, which causes the polymer concentration in the solution jet to rise sharply. The solution becomes more viscous and the voltage-induced stretch of the jet and polymer chains is reduced, as a result of which the fibers solidify rapidly and have a larger diameter [15]. However, for CA there is data suggesting the opposite – increasing humidity increases fiber diameters [21]. As electrospinning CA at ambient humidity creates the need for repetitive cleaning of the needle tip due to constant formation of large solution drop on the needle tip [22], increased humidity might be considered necessary for continuous and smooth electrospinning process.

An increase in temperature causes opposite effects - it increases the rate of evaporation of the solvent, but reduces the viscosity of the solution, which reduces the diameter of the formed fiber [17], [21]. Thus, a suitable combination of temperature and humidity

must be determined, at which the electrospinning process is continuous and without interruptions, yet smallest possible fiber diameters are obtained.

If the electrospinning solution has low conductivity levels, the droplet at the tip of the syringe does not have sufficient surface tension to form a Taylor's cone under the influence of an electric field, which in turn makes the electrospinning process unsuccessful. A similar problem arises with a solution that has conductivity above the critical limit, which prevents the Taylor's cone from being formed and thus no electrospinning process takes place [18].

### **2.1.2 Materials Used in Electrospinning**

Most electrospun materials are made of natural or synthetic polymers, but also metallic, bioactive, ceramic particles and other organic and inorganic materials can be added to the electrospinning system and thus be included in the composite nanofiber structure [14], [17]. The base polymer is mixed with a solvent to produce a homogeneous polymer solution. A second polymer can also be added to the base polymer solution, creating a hybrid nanofiber material. By including various additives in the electrospun material, the properties of the additives will also affect the overall properties of the electrospun nanofibrous material. For example, adding less than 10 wt% of commercial minerals to a polymer solution, helps create an electrospun material with significantly higher thermal resistance. Altering the electrospinning process itself can also have significant effect on the properties, structure and create new possible fields of applications of the electrospun material [23].

Electrospun materials can also be flexible, they can act as a passive supporting material such as a substrate or a template, or be used as an active material, like an electrolyte separator in an energy storage device [24]. As electrospinning is highly effective method to produce nanostructures, which also has many fields of scientific applications, such as supercapacitors, drug delivery systems and wound dressings, filtration devices, protective clothing development and biosensors [14], [17].

### **2.1.3 Biobased filter materials**

The majority of face masks found on the market today consist of fossil raw material-based polymers, such as polypropylene, polystyrene, polycarbonate, polyethylene, polyester [25]. As fossil materials are considered finite, finding more sustainable material alternatives is highly relevant [26]–[30]. Bio-based polymers are a promising

category of materials for that purpose, as their source material is biomass and thus can provide a more sustainable alternative to common polymers [26], [31]. Common bio-based polymers that can be electrospun include polylactides (PLA) [32]–[34], polyamides [35], [36] and cellulose acetate (CA) [26], [37], [38].

In the light of the global pandemic caused by the SARS-CoV-2 virus and the massive increase in face masks production, use and disposal [39]–[42], masks made out of polyethylene and polypropylene could pose a serious issue in the form of ocean pollution and remaining in landfills, even entering the human food chain as microplastic [43], [44]. Finding alternative materials to produce equally efficient yet biodegradable face masks has become increasingly important [45]. Thus, developing filter materials containing bio-based CA for face masks by the means of electrospinning has gained movement [45]–[48].

For electrospinning purposes, dimethylacetamide (DMAc) in combination with acetone have been used to create CA solution [49].

#### **2.1.4 Advantages and Uniqueness of Electrospinning**

Electrospinning has many advantages, like the overall simplicity of the process [16], [50], small fiber-to-fiber distance [51], its versatility, low cost [52], ease of surface modification [53]. Electrospinning enables the production of fibers with very small diameters, high surface area and with diverse structures, such as a smooth or porous surface, a hollow core structure, or a side-by-side fiber structure [18]. These characteristics add to the uniqueness of the electrospinning process, making it suitable for a diverse set of applications.

Electrospun material properties can be improved with additives such as nanoparticles [23]. The structure of nanofibers can also be altered with a variety of additives, such as thymol (C<sub>10</sub>H<sub>14</sub>O) [54], [55], [56]. Thymol is known for its antibacterial, antimicrobial, antifungal, as well as antiparasitic properties and it has been proven effective against *S. typhimurium*, *E. coli* and *S. aureus*. For electrospinning purposes, thymol is used to increase porosity for both electrospun CA nanofibers as well as nanofibers obtained by other methods [57]–[59]. Increasing nanofiber surface area by making it porous helps to ensure, that added nanoparticles are not encapsulated inside the fiber surface, to ensure maximum effect of nanoparticle properties [60].

## **Additives in Electrospinning Solutions and Their Use in The Medical Field**

Electrospinning process allows the use of electrospinning solutions with enhanced properties. Different additives can be added into polymer solutions to improve the properties of electrospun materials.

Using antimicrobial additives to create electrospun filter materials would improve its protective properties. Additives in the form of nanoparticles are preferred for electrospinning [61]–[65], because well dispersed nanoparticles reduce the risk of clogging the electrospinning needle. Nanomaterials, including nanoparticles have at least one dimension of 1-100 nm [49]

Antimicrobial substances are effective against a large variety of microorganism groups, such as bacteria, viruses, mold, algae and mildew. Antibacterial substances are effective against bacteria [66], [67]. Examples of antimicrobial nanomaterials, also known as nanoantimicrobials (NAMs), are transition metals, for example copper (Cu) and silver (Ag), as well as compounds of these transition metals [13]. Copper (Cu) itself has shown antimicrobial properties against a wide array of microorganisms such as *E. coli*, *Staphylococcus aureus*, and *Salmonella*. It is considered a cheaper option when compared to other metal elements with antibacterial properties such as silver [14][68]. Copper also has the ability to generate reactive oxygen species (ROS), which helps cause the death of microorganisms [69]. Copper has shown antibacterial properties, thanks to its ability to inactivate enzymatic pathways, generate ROS, damage bacterial proteins, modify the cell walls of bacteria and destroy or alter the synthesis of nucleic acids, without it becoming mutagenic. These advantages have led to its use in hospital surfaces [70]. Copper and copper alloy surfaces have proven effective against enveloped viruses like the coronavirus [68], [71]–[73], merely 5-minute exposure causing coronavirus infectivity to drop below detectable levels [68].

Copper oxide (CuO) has shown excellent antimicrobial properties, for example its suspension has shown antibacterial activities against pathogens like methicillin-resistant *Staphylococcus aureus* (MRSA) and *E. coli* [71], [74]. US Environmental Protection Agency (EPA) officially recognizes CuO as an antimicrobial material and it has been used as an additive in antimicrobial electrospun nanofibers [14] and as anti-microbial fabric treatments substance [49]. Basic copper carbonate ( $\text{Cu}_2(\text{OH})_2\text{CO}_3$ ) has also been applied as an antimicrobial agent [74].

Similar to CuO and  $\text{Cu}_2(\text{OH})_2\text{CO}_3$ , copper sulphate ( $\text{CuSO}_4$ ) salts have also shown excellent antimicrobial and antibacterial properties and it can be used against multi-drug resistant nosocomial pathogens [15]. Surfaces that have been coated with copper

sulphate or Cu, have demonstrated 90 to 95% less bacteria present. Like CuO, copper sulphate has also been effective against pathogens such as MRSA and *E. coli*, but also *Clostridium difficile*, among others [70]. Copper (II) hydroxide (Cu(OH)<sub>2</sub>) is used in the agricultural field for its antimicrobial properties [75], [76].

Ag compounds are commonly used to treat burns, wounds as well as infections, as Ag has very good antimicrobial properties against bacteria, fungi, algae and viruses. For this reason, Ag has many applications in the field of medicine throughout history [77].

The high surface area of Ag and CuO helps to intensify the antimicrobial properties of these substances [14], [77].

## **2.2 Studying and Altering Electrospun Materials**

### **2.2.1 Dispersion Analysis of Nanoparticle Additives**

For the added nanoparticles (NPs) and metal compounds to have maximum effect on the characteristics of the final product, homogeneous dispersion is required. However, this is still considered a problem in many areas using NPs, like coating, paints, inks, drug delivery, ceramic and nanocomposite processing. To study and analyse the size of metal clusters and NPs in polymer solutions, Dynamic Light Scattering (DLS) method is used. This method helps to examine the effect that many variables may have on the dispersion of the sample, such as solid concentration, surfactants and polymers [78].

NP clusters can also be studied with the use of Transmission Electron Microscopy (TEM). After the ultrasonication process is completed, a drop of the sample suspension is placed on a carbon film coated copper grid and dried at room temperature. The average cluster diameters are measured manually from the TEM images. Scanning electron microscopy (SEM) can also be used to study NP dispersion in suspensions [14].

Polydispersity index (PDI) is used to show the heterogeneity of a sample and its value is based on the size distribution of the particles. It can be used to determine agglomeration or aggregation. The exact value of PDI can be determined by different instruments such as dynamic light scattering (DLS) [78]. Maximum numerical PDI value is 1, which shows that the degree of non-uniformity within the sample is very large, which means the particles in the solution have very different sizes, which could be caused by agglomerates in the sample. The lowest possible PDI value is 0, which characterises a sample containing particles with extremely uniform sizes [79].



When metal compounds are added to base fluid, they form a nanofluid, which can be considered a colloidal solution [80]. Nanoparticles in nanofluids are prone to agglomeration, instead of fully dispersing in the base fluid. The size distribution of these agglomerates can vary on a large scale. This is due to a phenomenon called Brownian motion [81], which causes nanoparticles that are present in a stationary base fluid to move in a random and uncontrolled fashion, causing the particles to constantly collide with other molecules, particles [82] or agglomerates, resulting in the creation of agglomerates or clusters. The presence of nanoparticle agglomeration can be studied with the help of DLS, which enables to determine the size of the particles and thus also agglomerates that are present in the base fluid, as well as PDI [81].

### **2.2.2 Deacetylation Of Cellulose Acetate for Improving Hydrophilicity**

To achieve the protective properties of filter materials against viruses, the hydrophilicity of filter material is an important factor. Although cellulose diacetate has hydrophilic properties due to the hydroxyl group present in each glucose unit of its structure, increased hydrophilic properties could increase electrospun materials' suitability to be used as a filter material [83], especially in humid conditions caused by respiration [84]. Cellulose diacetate was treated with deacetylation for this purpose.

Hydrophilic membranes and filter materials are used in many applications, such as masks and other gas filtering systems, that have a tendency to develop condensation. Hydrophilic properties of the material help avoid possible contamination and other failures [85]

Studies have determined, that filters used in high humidity, such as masks which come in contact with humidity due to respiration of the wearer, have better filtration efficiency (of hygroscopic nanoparticles and respiratory droplets containing viruses, such as SARS-CoV-2) if the fabric is hydrophilic [84]. Higher hydrophilic properties also help lessen the time it takes for the droplets on and in the filter material to dry, which in turn helps to lessen the risk of the viruses reaching the wearer of the mask, as well as lessening the virus survival chances. Some sources claim, that droplets on hydrophilic filter materials dry four times faster than those on hydrophobic materials. Studies have also drawn the conclusion, that improving hydrophilic characteristics of filter materials that already have hydrophilic properties, can improve the filter materials anti-virus properties significantly [86].

To raise the hydrophilic properties of cellulose acetate, the process of deacetylation can be used. This process uses sodium hydroxide (NaOH) [87], which essentially replaces

the acetate groups of CA with hydroxyl groups, transforming cellulose acetate back to cellulose (Figure 2.3) [88], creating regenerated cellulose nanofiber material with excellent hydrophilic properties [89].

The reason why cellulose itself cannot be easily electrospun, is due to poor solubility of cellulose in common solvents, making it necessary to use cellulose derivatives for electrospinning purposes [90].

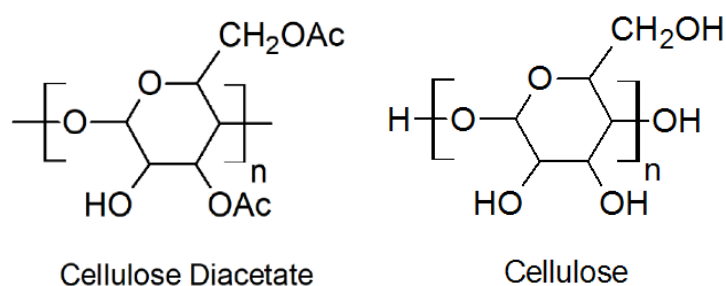


Figure 2.3 Cellulose diacetate [91] and cellulose comparison [92]

Deacetylation (Figure 2.4) can be done using 0.05M NaOH/ethanol alcohol (EtOH) (4:1) solution, which is added to the cellulose acetate sample. Deacetylation is done with ultrasound treatment for 1 hour at room temperature, with minimal solution to nanofiber mass ratio of 50:1. Once the deacetylation process is done, the hydrolysed sample is washed with deionized water. If necessary, the pH level of the sample might be tested after washing. Then the sample can be dried overnight in a vacuum at 60 °C [88], [93].

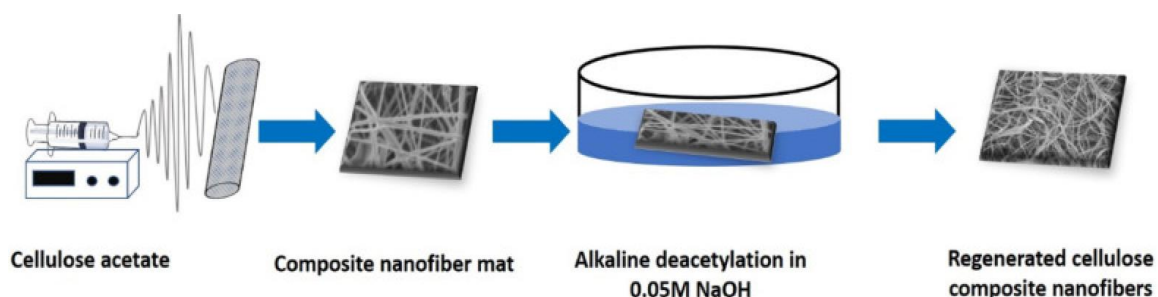


Figure 2.4 Deacetylation process [94]

Studies have shown, that the average fiber diameters of cellulose material, that was obtained after 1 h of deacetylation, remained very similar to the values of the cellulose acetate fibers, measured prior to deacetylation [88].

### 2.2.3 Fourier-Transform Infrared Spectroscopy

To determine the success of deacetylation, the regenerated cellulose nonwoven nanofibrous materials are known to be studied using Fourier-transform infrared spectroscopy (FTIR) [88]. The working principle of FTIR uses materials ability to absorb some of the infrared wavelength emitted by the FTIR machine, which then registers the spectrum of wavelengths emitted from the material, where some wavelengths have been absorbed by the material studied [95]. FTIR is used to determine the chemical structures or chemical changes in many fields, such as polymer science, pharmaceuticals, for analysing food and many more [96].

As can be seen in Figure 2.5, FTIR graphs of cellulose acetate and cellulose (for both pure cellulose or cellulose obtained by deacetylation of cellulose acetate) have some very clear differences, which can be used to determine the chemical composition of the material. For cellulose acetate, characteristic peaks are present at  $1745\text{ cm}^{-1}$  (stands for C=O),  $1375\text{ cm}^{-1}$  (stands for C-CH<sub>3</sub>), as well as  $1235\text{ cm}^{-1}$  (stands for C-O-C). As the acetate group is removed by the deacetylation process, these characteristic absorbance peaks are not present for the FTIR graph representing cellulose obtained by deacetylation of cellulose acetate [88].

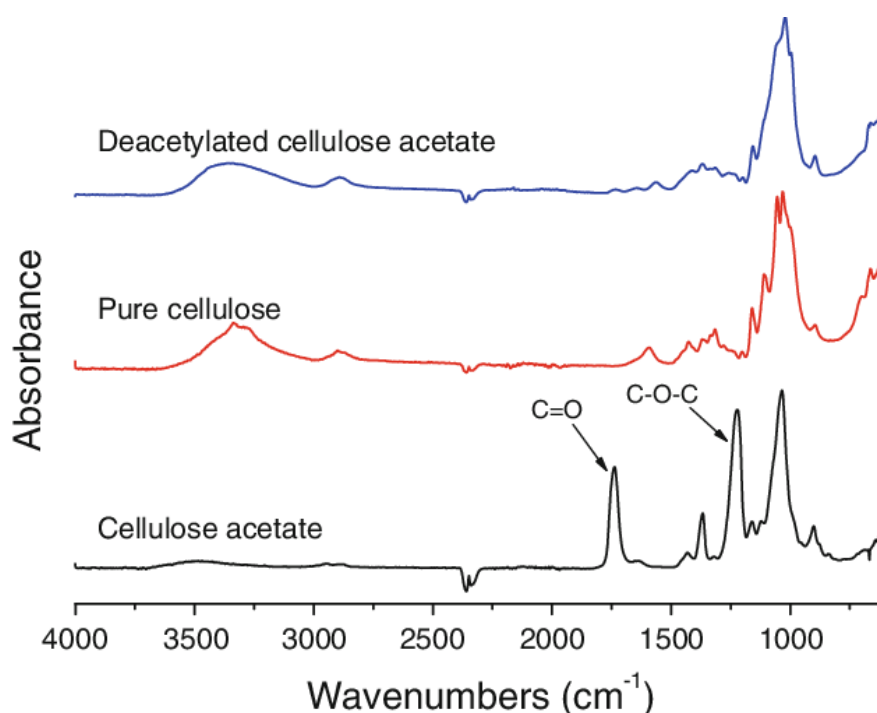


Figure 2.5 FTIR graph comparison for cellulose acetate, pure cellulose and deacetylated cellulose acetate (regenerated cellulose) [97]

Another way to determine the success of deacetylation with FTIR, is to look for the absorbance peaks of the hydroxyl group (-OH), that replace the acetate groups during the deacetylation process. As can be seen in Figure 2.5, both cellulose FTIR graphs have a rather flat, yet distinct arc in the region of 3200-3500  $\text{cm}^{-1}$ , which is not present for the cellulose acetate FTIR graph. This broad curve represents stretching of the hydroxyl groups, obtained by the deacetylation process [98]. Hydroxyl groups are known for their broad curves on the FTIR graphs, which make it easy to recognize. However, it has been noted that hydroxyl groups absorb differently depending on their environment [99].

## **2.3 Air Filter Materials**

### **Airborne particles**

Air filtration is the most commonly used technology to remove airborne particles from air [100]. These particles include airborne bacteria and viruses, which have recently become a serious concern on a global level. It has also been noted that spreading of viruses is directly linked to air pollution, which in itself is a great challenge of this century [1]. Viable aerosolized virus particles can be as small as few nanometres and they are created when an infected person sneezes or coughs, or by an air flow that helps the virus particles become airborne from a contaminated surface [101]. Small airborne virus particles can be transported to other locations with airflow. When inhaled, small virus particles can be easily transported into lower lungs which can cause worse outcomes, compared to virus particles that remain in the upper respiratory tract once inhaled [101], [102].

Airborne virus particles of influenza or upper respiratory tract infection range between  $<0.1 \mu\text{m}$  to  $10 \mu\text{m}$  and the highest particle concentration was in the range of  $0.35\text{--}2.5 \mu\text{m}$  [14], [104], [105]. Studies of COVID-19 patients have shown that  $7.18 \times 10^{-4} \%$  of respiratory fluid particle from the infected patients contained SARS-CoV-2, smallest possible respiratory particle size that is able to contain SARS-CoV-2 was estimated as  $4.7 \mu\text{m}$  [103], [106] and aerosol particles containing SARS-CoV-2 remain airborne for hours, which is significantly longer than that of other respiratory infection aerosol particles [106], [107].

### **Viruses**

The filtration efficiency of filter material is closely linked with the structure of airborne particles, such as viruses and microbes, and their work mechanism. Thus, it is essential to have an overview of its parameters, including the structure of the particle, its surface coating, its size and shape [108].

Virus consists of DNA or RNA surrounded by protein. Although it contains genetic code, it is unable to replicate by itself, they rely on infecting host cells by penetrating them, and using the host to replicate, after which the host cell is killed [109], [110], [111]. Viruses are significantly smaller than bacteria, for example the hepatitis virus is about 45 nm, which is approximately 40 times smaller than *Escherichia coli* (*E. coli*). Viruses gain access to the host organism by the means of open wounds, bug bites and respiratory passages [112].

The severe acute respiratory syndrome coronavirus 2 (SARS-CoV-2) particle (Figure 2.6) consists of a core containing RNA polymers, which is surrounded by nucleocapsid protein molecules. The core of RNA and nucleocapsid molecules is covered by a membrane, containing envelopes of hydrophobic lipids with hydrophilic proteins [110], [113], [114]. The membrane of the coronavirus particle is covered in spike proteins [110]. These proteins are covered with polysaccharides, helping to hide the virus particle from the immune system of the host [102]. The outer layer of the virus particle can be considered hydrophobic with varying degrees of hydrophilic properties added due to the structure of the glycoproteins on the outer surface [102], [115].

## Coronavirus Structure

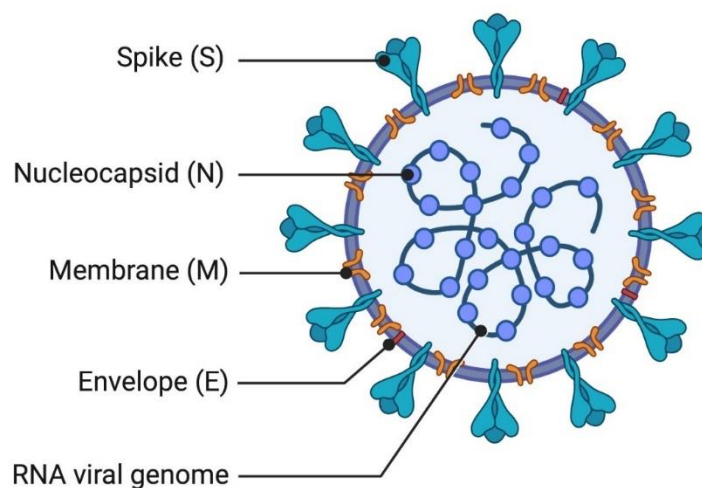


Figure 2.6 The structure of the SARS-CoV-2 virus [110]

During the worldwide pandemic which started in December 2019 [3], [103], [116], notable effort has been made to reduce the spread of SARS-CoV-2 and COVID-19. The main way of transmission for the virus is considered to be airborne respiratory particles

(<5–10 µm diameter) produced by infected subjects [103]. SARS-CoV-2 particle size has been determined to fall in the range of 50-140 nm [117].

As with all RNA viruses, new variants of SARS-CoV-2 are emerging constantly, with each being more easily spreading than the previous variant, especially the Delta and Omicron variants [118], [119]. The resistance to vaccines, rate of spread and severity [2]–[4] of RNA viruses is unpredictable, thus using masks is critical for preventing the spread of SARS-CoV-2 [5] [2]. Easier transmission of SARS-CoV-2 might be caused by its spikier outer coating proteins (Figure 2.6), which attaches the virus tightly to the cells in lungs, nose or other body parts of humans. Mutations with spikier outer proteins are able to make a tighter connection with the cells [2].

As SARS-Cov-2 virus is considered transmissible by air, particulate matter (PM) could potentially create favourable means of transportation to it, that could exceed the commonly accepted close contact distance of 2 metres (m). As PM in itself has been the cause of lung inflammation, the effects of PM combined with COVID-19 could prove to be much more severe [1].

### **2.3.1 Air filtration mechanisms**

Air filtration can be divided into two main states – steady state and non-steady state. Steady state, which is also known as the first state, has a constant efficiency rate of particle capture and filtration pressure drop level, as its efficiency only depends on the properties of the filter material, particles and the air flow. The steady state can be subdivided into five different mechanism types, which are interception, inertial impaction, Brownian diffusion, the electrostatic effect and the gravity effect [7]. For the non-steady state, which is also known as the second state, the flow resistance and overall efficiency change over time, as the filter material surface becomes saturated with filtered particles [7].

## **Air filtration systems and methods**

Air filtration systems use materials that can be divided into two main groups - fabric and fibrous filters. Fabric filters collect airborne particles on the surface of the filter and they are primarily made of felted woven fabrics. Fibrous filters collect airborne particles throughout the cross-section of the filter instead of the surface. They are made of a nonwoven material that in turn consists of individual fibers, which are oriented randomly while being perpendicular to the air flow. Fibrous filters use fibers with diameters as small as 1 micrometre ( $\mu\text{m}$ ) to as large as hundreds of micrometres, which can be made from many different materials, such as fiberglass and polymers [100].

In recent years, electrospinning has been studied as a potential method to produce nanofibrous air filter materials [6]-[10], [120]. Electrospun nanofibrous membranes (ENMs) have a delicate structure and as filter materials have many different fields of application to them, such as air filtration or general filtration systems (for example biotreatment sewages), medical field and energy. The reason for this is the great performance of nanofibers in air filtration, they also have good surface-to-volume ratio [9], small diameters and have the ability to incorporate necessary additives [7]. Nanofibers have also shown exceptional results in removing airborne viruses, nanoparticles (NPs), bacteria as well as volatile organic compounds (VOC) from filtered air [6][12]. This is due to the combination of Brownian diffusion and interception [9].

Main characteristics of electrospun filter materials are air permeability [ $\text{mm/s}$ ], filtration efficiency [%] and pressure drop [ $\text{Pa}$ ] [9].

It has been noted that lower fiber diameter means improved filtration efficiency. This is due to the size of the particles that are being collected - submicron particles are easier to catch with nanofibers than with larger ones [19]. Porosity of nanofibers is also known to improve the air filtration properties of the electrospun material [121]-[123]. Polymer concentration in the electrospinning solution has an essential role to play in affecting the filter materials fiber diameters. The higher the polymer concentration in solution, the thicker fibers are achieved, thus minimal polymer concentration should be chosen in order to achieve small diameters. Still, the polymer concentration should be as high as necessary to guarantee the development of Taylor's cone on the needle tip. Flow rate also plays an important role in changing the fiber diameter - the higher the flow rate, the smaller the fibers. The reason for this lies in viscosity reduction with rising shear rates. The needle generates lower resistance to stretching with higher speed and fiber diameter is reduced while it travels between the tip and the collector [17], [124]. For producing electrospun nanofiber filter material, using a substrate material is required, nonwoven fabrics are especially widely applied for this purpose [125]. Electrospinning

nanofiber filter materials can be made of polyacrylonitrile, polycaprolactone, polypropylene, polyvinylidene fluoride [7], [126], polyvinyl alcohol [127] as well as cellulose acetate [9].

### **2.3.2 Electrospun filter materials in medicine field**

Personal protective equipment (PPE) is used in the medical field to prevent the spread of microbes, including bacteria, viruses, fungi, which cause infections and diseases [128], [129] and protect health care workers and patients [130]. PPE is also used to reduce the risk of transmitting health care workers' microorganisms onto patients. PPE includes a variety of masks such as surgical masks or respirator masks, also gloves, aprons, long sleeved gowns, goggles and face visors [131].

Electrospun materials can have many applications in the medical field, such as electrospun protective materials for antiviral protection, which can be used to produce surgical gowns with both passive and active protective properties [126], [132] as well as face masks for filtration purposes [133]. Electrospun materials can also be used for virus detection as well as drug encapsulation and delivery [126].

PPE usually has various standards and regulations for its design and manufacturing. Some of these regulations that specifically apply to disposable masks include the wearer's ease and ability to breathe while wearing the mask, as well as the fit and overall comfort of the mask. As these disposable masks are meant to be used once and then disposed of, it is sensible for the manufacturing levels of these PPEs to be as low as possible [134] or to use biodegradable materials to produce PPEs [45].

In terms of efficiency of disposable masks and more specifically the filter materials used in them, smaller fiber diameters have shown improved filtration capabilities compared to the results of increased fiber diameters [15]. To achieve the smallest possible diameter for any electrospinning system, the parameters of the electrospinning process and the corresponding fiber diameters are statistically analysed and the parameters with the best results are determined [135]. With this correlation in mind, filters consisting of electrospun nanofibers have shown excellent results as high efficiency particulate air (HEPA) and ultra-low penetration air (ULPA) filters [15]. HEPA and ULPA filters are both used to remove particles as small as 0.1  $\mu\text{m}$  (ULPA) and 0.3  $\mu\text{m}$  (HEPA) from air [136].



## 3. EXPERIMENTAL PART

### 3.1 Materials and Methods

#### Materials

Cellulose acetate (CA), purchased from Sigma-Aldrich, with average Mn ~30,000 by GPC, impurities  $\leq 3.0\%$  water, has been chosen as a polymer matrix to produce filter materials with enhanced protective properties by electrospinning method. Acetone (Honeywell, assay (GC)  $\geq 99.5\%$ ) and dimethylacetamide, DMAc, (Sigma-Aldrich, ReagentPlus®, assay (GC)  $\geq 99\%$ ) were used to prepare the mixture of the solvents in ratio of 2:1 for polymer electrospinning solutions based on literature data results [137]. To increase protective properties against viruses and microbes, the following additives were used – copper oxide (CuO) from Sigma-Aldrich, copper sulphate (CuSO<sub>4</sub>) from Alfa Aesar, basic copper carbonate (Cu<sub>2</sub>(OH)<sub>2</sub>CO<sub>3</sub>), copper (II) hydroxide (Cu(OH)<sub>2</sub>) as well as silver (Ag) from Sigma-Aldrich. Also, the combination of several nanoparticles in one solution was used to increase the protective properties. Thymol (Fisher Scientific) was used as a special additive in the polymer solutions to increase the porosity of electrospun materials. The choice of thymol was based on the literature data [57].

#### Methods

##### Polymer solution preparation

All base polymer solutions were prepared with CA concentration of 17 wt% and the concentration of polymer matrix did not change. The weight concentration method was used (3.1).

$$C = \frac{m_{solute}}{m_{solution}} * 100 \quad (3.1)$$

where  $C$  – weight concentration, %

$m_{solute}$  – mass of solute, g

$m_{solution}$  – mass of solution, g

The polymer solutions were prepared by mechanical mixing using a magnetic stirrer at room temperature for 24 hours to achieve homogeneity of solution.

The concentrations of the additives used were calculated on the dry matter in the polymer solution. The additives concentrations were chosen basing on the viscosity of the polymer solution to achieve successful electrospinning, but no less than that one to

achieve the copper, Cu, concentration in the chosen additive to be 7,5%. The used solutions are presented in Table 3.1.

Table 3.1 Electrospinning polymer solutions (17% CA in Acetone-DMAC mixture) with additives used in the study

No	Nominal concentration of additives, %	Nominal content of pure Cu in the solution, % (calculated)
1	(Reference solution, without additive)	-
2	18.75% CuSO <sub>4</sub>	7.5
3	12.5% CuO	10
4	18.75% CuSO <sub>4</sub> + Ag ( <b>1/8</b> of CuSO <sub>4</sub> mass)	7.5
5	18.75% CuSO <sub>4</sub> + Ag ( <b>1/4</b> of CuSO <sub>4</sub> mass)	7.5
6	9.5% Cu(OH) <sub>2</sub>	7.5
7	14.7% Cu <sub>2</sub> (OH) <sub>2</sub> CO <sub>3</sub>	7.5
8	10% Thymol in reference polymer solution (without any metal compound additive)	-
9	18.75% CuSO <sub>4</sub> and 10% thymol	7.5

### Ultrasound method

To achieve the dispersion of the additive in basic polymer solution the treatment by ultrasound was done using Branson Digital Sonifier 450 device. Firstly, the additive was dispersed in DMAc solvent by ultrasound for 45 min. When the dispersion was ready CA and acetone were added and mixed mechanically by magnetic stirrer at room temperature for 24 h. Acetone was added in the final stage of preparation process to avoid the evaporation of the volatile solvent from the polymer solution.

### Electrospinning

Electrospinning was performed by using a handmade set-up (Figure 3.1) at room temperature and air humidity of 60% (relative humidity, RH) [138]. It was observed, that lowered humidity levels caused noticeable fluid build-up at the tip of the needle. The same was not observed with 60% humidity while using the same pumping rate. This observation is confirmed by literature, where similar fluid droplet build-up was observed in ambient humidity [22]. However, electrospinning in the presence of too high humidity, might result in deposition of wet fibers that fuse together before drying [21].

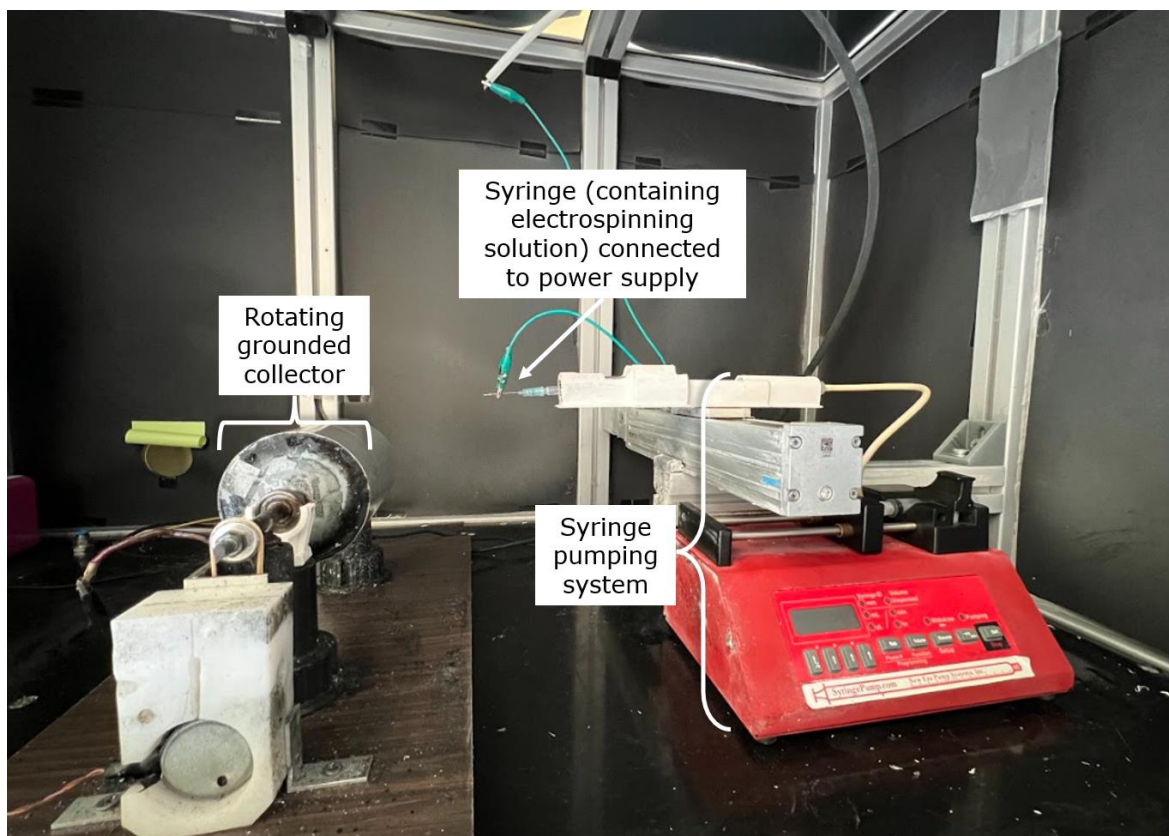


Figure 3.1 Electrospinning setup

Electrospinning of all solutions was performed using a syringe with 0.4 mm diameter needle, distance between the needle tip and collector of 15 cm, voltage of 10-15 kV and pumping rate of 0.2-0.9 ml/h. The choice of electrospinning parameters was dependent on the electrospinning solution properties, such as viscosity and used additives. Achieving proper nanofibrous morphology of the electrospun materials was required, process parameters were chosen accordingly to meet this goal. The electrospinning solution amount was calculated and electrospun in such a way that all produced materials had the most similar thickness.

### **Dispersion Analysis of Additives**

Sufficient dispersion of additives is an important factor for the creation of stable nanofluids containing well dispersed additives [139]. Additives such as NPs prone to agglomeration will most likely be distributed unevenly throughout the electrospun fibers and subsequently cause other issues in the electrospinning process, like blocking of the needle [16]. Agglomeration of additives in the solvent system could be caused by the additives' aim of reducing free energy, resulting in particles of varying sizes [140]. Dispersion analysis of the solutions with additives was used to estimate the compatibility of the additive with the chosen solvent system. Same additive concentrations were used,

as in the electrospinning polymer solutions. Then the solutions were diluted 20 times in order to achieve accurate measurement results [141]. Dispersion was examined with Malvern DLS instrument, which studies the Brownian motion of particles in suspension and deduces particle sizes and size distributions based on velocity of the particles, enabling dispersion and agglomeration estimation [136].

### **Scanning Electron Microscopy (SEM)**

Hitachi TM-1000 Tabletop Microscope SEM device was used to estimate the morphology of electrospun materials and to measure the fibers' diameter. An advanced SEM device was used to study the electrospun fibers surface in greater detail to analyse morphology and porosity changes caused by the addition of thymol.

### **Thickness of Electrospun Filter Material**

The thickness of the electrospun filter materials was measured with Sony thickness measurement device. The measurements were done in eight different places and the average thickness was calculated. The thickness of the substrate material was considered in the electrospun material thickness calculation. The thicknesses of all produced electrospun materials were 0.017 – 0.163 mm.

### **Air Permeability Testing**

Air permeability analysis is significant in filter material characterization. Prior to the air permeability testing, test specimens were preconditioned at temperature of  $20 \pm 2$  °C and air relative humidity of  $65 \pm 4$  % for 24 hours to achieve uniform humidity of the materials [142] according to ISO 139:2005 [143]. Air permeability was estimated using FX 3340 MinAir device, which draws air through the sample at a constant rate and measures the air exchange pressure of the sample. Air flow speed during these tests was 8 l/min, test area was 4.9 cm<sup>2</sup>.

To study the air permeability, also known as breathability, a device capable of measuring differential pressure needed to draw air through the sample at a constant air flow is required. This device then measures the air exchange pressure of the mask. Water based or digital manometer in combination with a mass flow meter can be used for this purpose [142].

### **Aerosol Filtration Efficiency**

Aerosol filtration efficiency is a highly important characteristic of filter materials. Estimation of the aerosol filtration efficiency of electrospun filter materials was done at Estonian Environmental Research Centre (EKUK) according to EVS-EN 13274 and ASTM F2299/F2299M. Polydisperse aerosol with particle range of 11.8-429.4 nm was used in

this test, covering the 300 nm particle size which N95 masks are certified to filtrate [144]. Scanning Mobility Particle Sizer (SMPS) TSI model 3082 and Condensation Particle Counter (CPC) TSI model 3775 were used to determine the aerosol concentration before and after passing through the electrospun materials. Aerosol filtration efficiency was calculated using formula 3.2.

$$eff = \frac{C_a - C_p}{C_a} * 100 \quad (3.2)$$

where *eff* – filtration efficiency, %

$C_a$  – aerosol concentration before passing through electrospun material, #/cm<sup>3</sup>

$C_p$  – aerosol concentration after passing through electrospun material, #/cm<sup>3</sup>

### **Contact angle measuring**

To estimate the hydrophilicity or hydrophobicity of the produced electrospun filter materials contact angle was measured by using Sessile drop method [145], [146] with the device DataPhysics OCA 20 and SCA 20 software. Distilled water was used as a liquid agent to create the drop on the measured surface of the material. All measurements were performed at room temperature and the air humidity of 40%.

### **Deacetylation Of CA Electrospun Materials**

To raise the hydrophilic properties of cellulose acetate, the process of deacetylation was used [87]-[89].

Electrospun materials were deacetylated by mixing 1-part EtOH with 4 parts of alkaline 0.05M NaOH solution and submerging the cellulose acetate material in this mixture. Deacetylation with ultrasound treatment was done for 1 hour. The solution amount was selected based on the size of the container, in order to fully submerge the sample. After deacetylation, the hydrolysed samples were carefully rinsed with distilled water. The washed samples were dried in the vacuum oven at 60 °C for 24 hours.

### **Fourier-Transform Infrared Spectroscopy (FTIR)**

To determine the success of deacetylation, the regenerated cellulose nonwoven nanofibrous filter materials were analysed using the Interspec 200-X FTIR Spectrometer.

### **Metal Test**

Determining the amount of metal particles in electrospun filter materials, X-ray analytical instrument S2 PICOFOX was used. The working principle of this device uses X-ray excitation to identify substances based on the specific energy level of substances, which is expressed by measuring the fluorescence of that substance. Electrospun material with known dimensions is cut and dissolved in HNO<sub>3</sub>. The diluted solution is applied to a polished sample carrier and dried until a thin film is created, creating a test specimen which is then analysed for metal concentration.

### **Microbiological Test (Agar Diffusion Assay)**

To determine the effect of the additives of copper compound on the increasing of protective properties of the electrospun material, antibacterial properties against Gram-negative *Escherichia coli* (*E.coli*) and Gram-positive *Staphylococcus aureus* (*S.aureus*) were studied [147], [148]. The choice of *E.coli* and *S.aureus* was also based on the pathogenic strains of these bacteria being the cause of infections in hospitals, *E.coli* and *S.aureus* have also shown resistance to antibiotics [149]. Typical microbiological test to determine the antibacterial properties against *E.coli* and *S. aureus* includes overnight cultivation of the bacteria, followed by incubation in the nutrient broth, causing the bacteria to grow. The suspension of bacteria in a specific concentration is then spread on a LB agar Petri dish. Samples of the electrospun filter materials are placed onto the Petri dish for 24 hours and kept at 37 °C for incubation. The antibacterial properties are estimated by visual inspection of the growth of the bacteria on the surface of the electrospun materials.

### **Antiviral efficiency test (Plaque Assay)**

Electrospun filter materials were tested against SARS-COV-2 in collaboration with Professor Andres Merits group at University of Tartu, testing was done by Associate Professor Eva Žusinaite. Human coronavirus SARS-CoV-2 propagated from a qPCR-positive sample was used with Vero-E6 cell line (the cell culture library of University of Tartu Institute of Technology) and was grown in a virus growth medium. After incubating, the virus was titrated by plaque assays. To analyse the antiviral efficiency of additives used in electrospun filter materials, 2x2 cm sized material pieces of select samples were evaluated with weight difference less than 10%. The virus titers were then calculated at 0-h time as well as at 1-h time point.

## 3.2 Results and discussion

### 3.2.1 Dispersion Analysis of Additives

Additive dispersion was examined with Malvern DLS instrument, overview of the results can be seen in Table 3.2.

Table 3.2 Dispersion estimation of additives based on DLS test results

No	Additive	Dispersion
1	CuSO <sub>4</sub>	Dispersed, minimal precipitation
2	CuO	Dispersed
3	CuSO <sub>4</sub> + Ag	Dispersed, minimal precipitation
4	Cu(OH) <sub>2</sub>	Dispersed
5	Cu <sub>2</sub> (OH) <sub>2</sub> CO <sub>3</sub>	Well dispersed

Addition of NPs to CA solution mixture presented no significant agglomerates, however the mixture with CuSO<sub>4</sub> did show some precipitation. This was successfully removed by ultrasound sonication mixing for 30 minutes. Basic copper carbonate Cu<sub>2</sub>(OH)<sub>2</sub>CO<sub>3</sub> presented promising results, having the smallest average particle diameter of 265 nm and lowest PDI value of 0.256, which is most likely linked to the lowest number of agglomerates.

All of the tested compounds and NPs were dispersed in electrospinning solutions and electrospun into filter material, in order to further study their suitability as additives for filter materials with enhanced protective properties.

### 3.2.2 Electrospinning of filter materials

The success and possibility of electrospinning CA polymer solution with different additives to produce filter materials with enhanced protective properties were estimated on a SEM analysis. The results of SEM images with the measured fiber diameters are demonstrated in Table 3.3.

From Table 3.3 it can be seen that the morphology of the electrospun materials is smooth without large agglomerates. It indicates that the added nanoparticles and copper compounds are well dispersed into the polymer solutions. The fibers have random orientation with average diameter from 463 nm up to 913 nm. From Table 3.3 it can be observed that the variability in fiber diameter depends on the copper

nanoparticles added into CA polymer solutions. Thus, the filter material electrospun from the pure CA solution shows one of the smallest average fiber diameters of 470 nm (a). Presence of additives causes the average diameter to increase. The increase may be explained with the size of nanoparticles added and the dispersion level achieved in the polymer solution, as using NP additives can increase fiber diameters of electrospun materials [150], [151]. From the images d, e, f of Table 3.3 the decrease of fiber diameter with some agglomerates can be seen. It can be explained by using one more additive of silver (Ag) in the polymer mixture that is not well dispersed in the solution and shows precipitation (d, e). The same is demonstrated in the morphology of the electrospun material with added copper hydroxide, 9.5%  $\text{Cu}(\text{OH})_2$  (f). Some sources claim that beaded nanofibers are best for creating deep filtration instead of surface filtration. Because surface filtration is usually characteristic to nanofibrous filters, and as the presence of beads or particles could improve the deep filtration properties of the materials, these materials could have significantly improved filtration capabilities [152]. However, there is no distinct correlation between the distribution of fiber diameters and materials antimicrobial values or air permeability which would impact the materials success as filtering material, as will be discussed in following chapters.

Table 3.3 figure g shows fibers of material containing  $\text{Cu}_2(\text{OH})_2\text{CO}_3$  with distinct grooves on their surface. Materials with  $\text{CuSO}_4$  and Ag additives (d-e) as well as only  $\text{CuSO}_4$  additive (b) also have slightly grooved surfaces. Grooved fibers are known to have improved filtration efficiency, compared to smooth fibers [153], [154]. As no pattern in the electrospinning process parameters of these materials compared to smooth fiber materials can be drawn, the cause for fiber surface structure changes lies in the additives themselves.



Table 3.3 SEM images and average diameters of electrospun filter material fibers

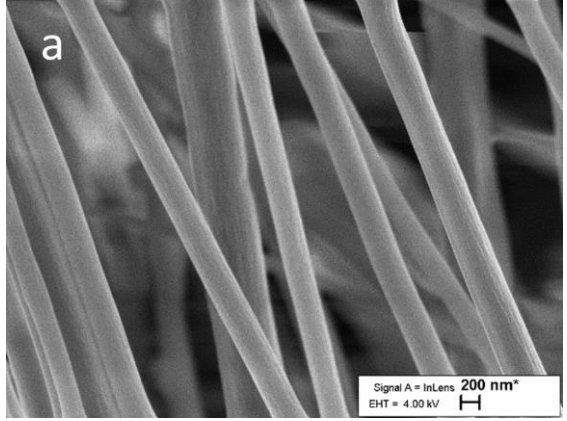
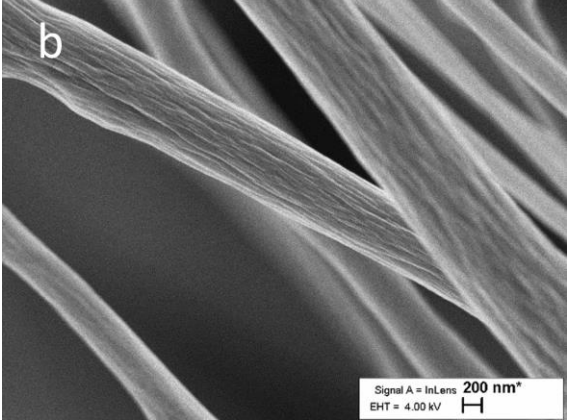
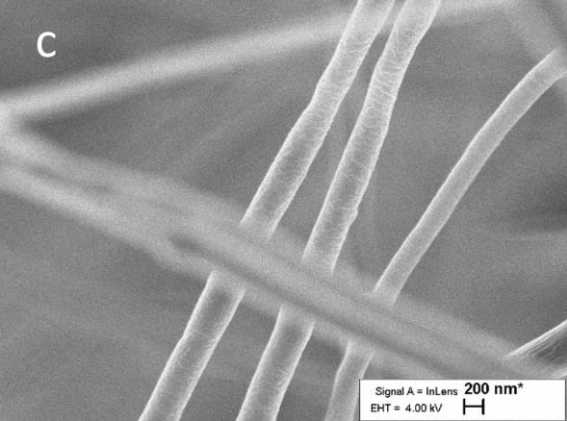
No	Additive	SEM
1	-	 <p data-bbox="979 763 1305 797"><math>d_{av} = 469.50 \pm 123.66 \text{ nm}</math></p>
2	18.75% CuSO <sub>4</sub>	 <p data-bbox="979 1279 1305 1312"><math>d_{av} = 519.31 \pm 201.95 \text{ nm}</math></p>
3	12.5% CuO	 <p data-bbox="979 1800 1305 1834"><math>d_{av} = 463.19 \pm 144.76 \text{ nm}</math></p>

Table 3.3 continued

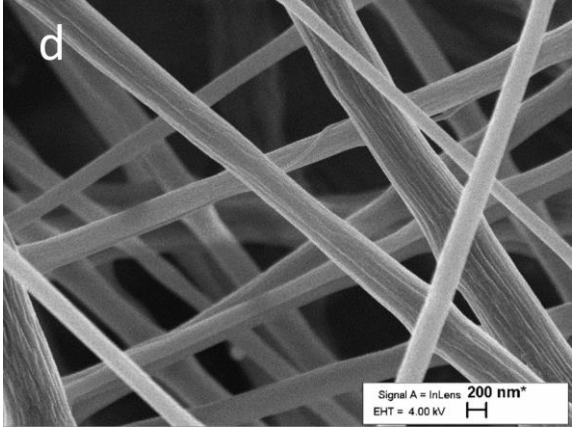
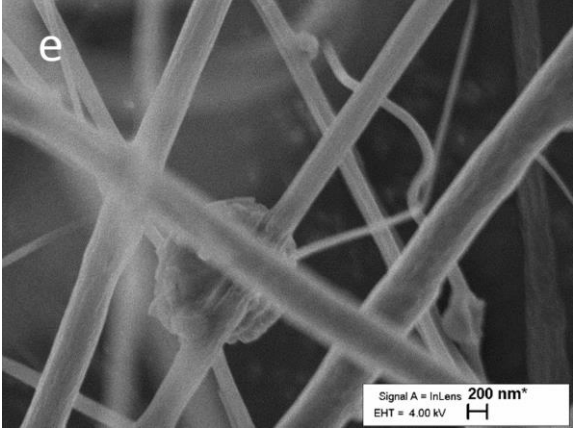
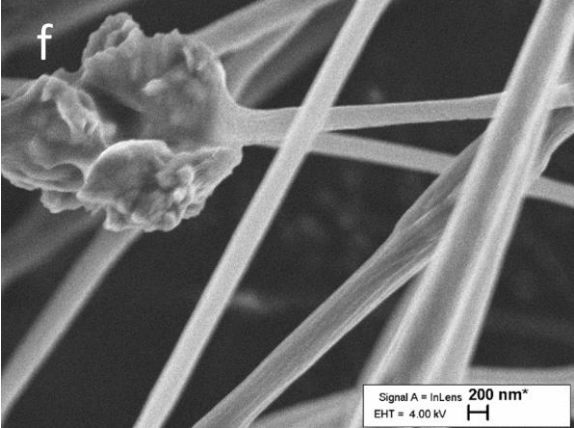
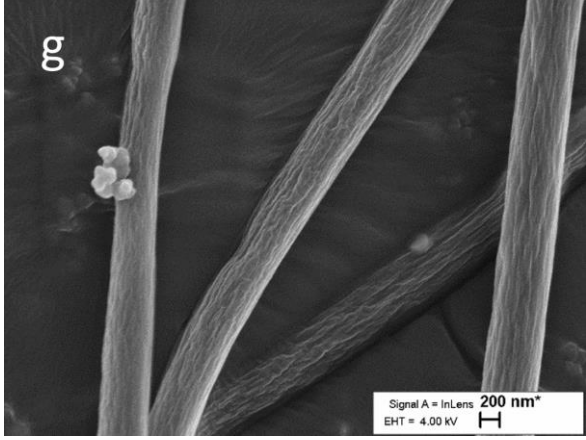
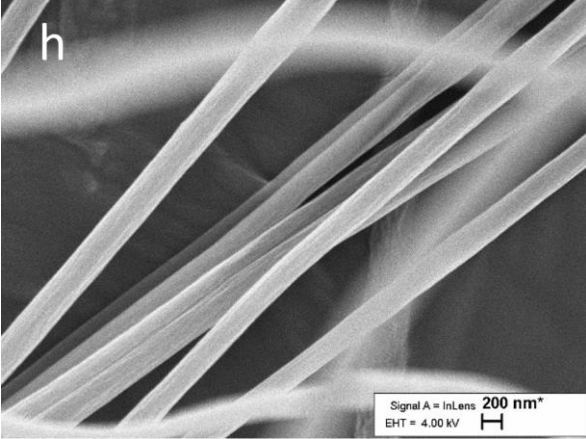
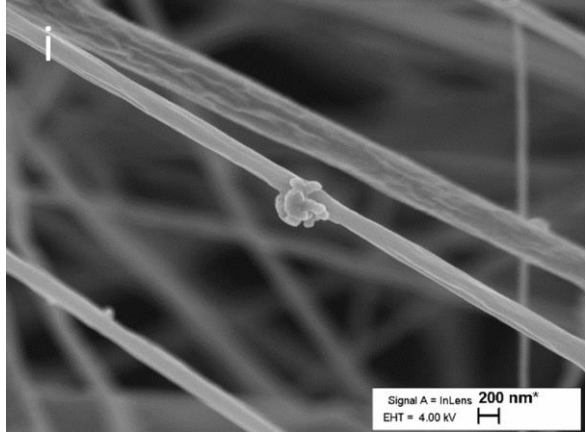
No	Additive	SEM
4	18.75% CuSO <sub>4</sub> and Ag (1/8 of CuSO <sub>4</sub> mass)	 <p data-bbox="979 775 1305 801"><math>d_{av} = 913.38 \pm 327.31 \text{ nm}</math></p>
5	18.75% CuSO <sub>4</sub> and Ag (1/4 of CuSO <sub>4</sub> mass)	 <p data-bbox="979 1296 1305 1323"><math>d_{av} = 603.77 \pm 179.88 \text{ nm}</math></p>
6	9.5% Cu(OH) <sub>2</sub>	 <p data-bbox="979 1818 1305 1845"><math>d_{av} = 637.47 \pm 135.01 \text{ nm}</math></p>

Table 3.3 continued

No	Additive	SEM
7	14.7% $\text{Cu}_2(\text{OH})_2\text{CO}_3$	 <p data-bbox="836 344 863 389">g</p> <p data-bbox="1177 707 1342 741">Signal A = InLens 200 nm* EHT = 4.00 kV</p> <p data-bbox="986 781 1299 815"><math>d_{av} = 613.39 \pm 85.30 \text{ nm}</math></p>
8	10% thymol	 <p data-bbox="836 878 863 922">h</p> <p data-bbox="1177 1240 1342 1274">Signal A = InLens 200 nm* EHT = 4.00 kV</p> <p data-bbox="978 1314 1307 1348"><math>d_{av} = 511.78 \pm 145.42 \text{ nm}</math></p>
9	18.75% $\text{CuSO}_4$ and 10% thymol	 <p data-bbox="836 1411 863 1456">i</p> <p data-bbox="1177 1774 1342 1807">Signal A = InLens 200 nm* EHT = 4.00 kV</p> <p data-bbox="978 1848 1307 1881"><math>d_{av} = 481.67 \pm 103.97 \text{ nm}</math></p>

As expected, adding NPs and metal compounds to the electrospinning solution results in some structural change in the materials general appearance, as for example NPs appear on the surface of the fibers.

Thymol was used as an additive to improve the porosity of electrospun filter material [55], [60], which is confirmed by the SEM images (h, i).

The fiber diameter values of most of the electrospun filter materials are suitable for air filtering purposes as they are suitably small. As mentioned in a previous chapter, lower fiber diameter can also improve the filtration efficiency of the material. This is due to the size of the particles that are being collected - submicron particles are easier to catch with nanofibers than with larger ones [19]. Based on this, electrospun filter materials containing  $\text{CuSO}_4$  and Ag NP additives show the poorest results, having the largest fiber diameters. All other electrospun filter materials have similar fiber diameters, suitable for filtering purposes.

As previously mentioned, materials with grooved fiber surfaces are most suitable for filtration purposes. Based on the SEM images, it can be concluded that materials containing  $\text{Cu}_2(\text{OH})_2\text{CO}_3$ ,  $\text{CuSO}_4$  and Ag additives are the best for this reason, as they have the most grooved fiber surface morphologies. As low fiber diameters are excellent for filtration of submicron particles, it can be concluded that the materials containing no additives,  $\text{CuSO}_4$  or  $\text{CuO}$  additives have the best test results in this area. Because the material containing  $\text{Cu}_2(\text{OH})_2\text{CO}_3$  NPs has middling fiber diameters compared to other electrospun filter materials and its fibers have grooved surface morphologies, this electrospun material has the best overall properties for filtering purposes based on SEM analysis.

### **3.2.3 Analysis of Hydrophilic Properties of the Electrospun**

#### **Materials**

The hydrophobicity may have a significant effect on the microbiological protective properties of the filter materials, especially against SARS-CoV-2 with its hydrophobic lipid bilayer envelope [114], [155]. As mentioned in previous chapters, filters used in high humidity have better filtration efficiency and lower the virus survival chances if the fabric is hydrophilic [84][86]. Hydrophilicity is also known to improve the bioactivity of antimicrobial polymers. Thus, the best result for antimicrobial properties would be to achieve a balance between hydrophobic and hydrophilic properties for polymers [156].

In the present study, the contact angle of the electrospun filter materials was measured to estimate the hydrophobicity/hydrophilicity. Contact angle measurements above the 90° threshold level shows hydrophobic properties of the material, whereas contact angle below 90° means that the material is hydrophilic [157], [158]. The results are presented in Figure 3.2-3.3 and Table 3.4.

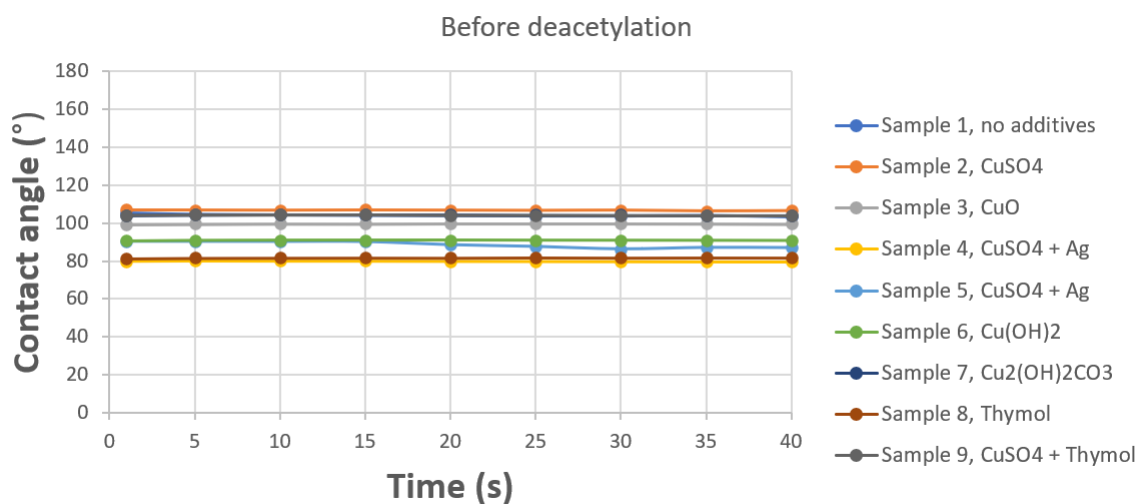


Figure 3.2 Contact angle measurements before treatment by deacetylation

As presented in Figure 3.2, electrospun filter materials before treatment by deacetylation have very uniform contact angle measurement results throughout the 40 second testing time frame, presenting mainly hydrophobic properties. The only electrospun materials which have hydrophilic properties before the treatment by deacetylation are the ones containing hydrophilic Ag nanoparticles [159] (Samples 4-5) and thymol (Sample 8), which has both hydrophobic and hydrophilic properties [160].

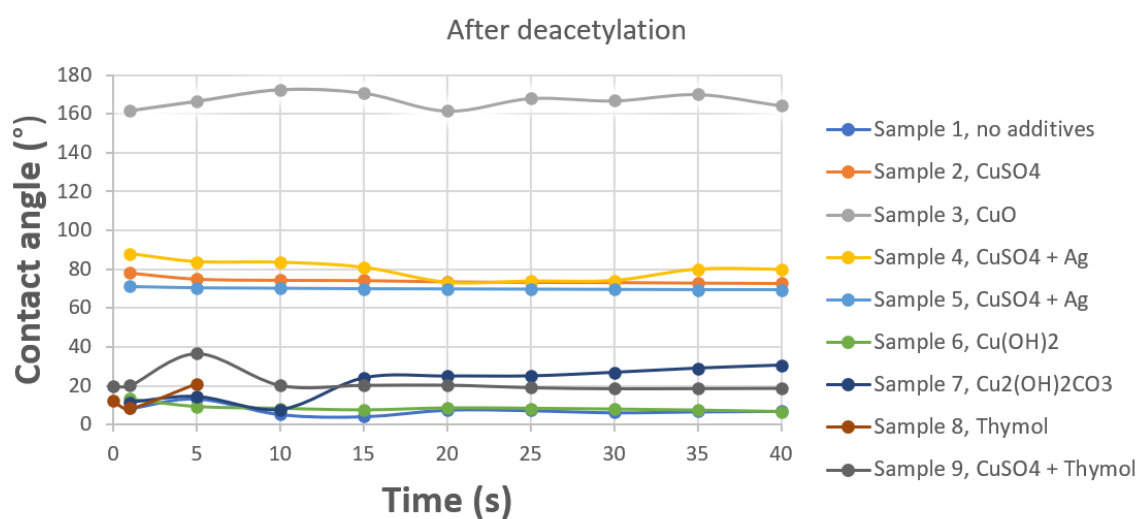


Figure 3.3 Contact angle measurements after treatment by deacetylation

As presented in Figure 3.3, all of the electrospun materials have changed into hydrophilic by deacetylation, except Sample 3 with CuO nanoparticles added. However, as success of deacetylation was determined by FTIR analysis, as will be discussed in a following chapter, the most likely cause for this phenomenon is hydrophobicity of CuO itself [161], [162]. As shown in Table 3.4 in metal content quantification chapter, CuO NPs had the highest measured metal concentration of all additives, which is the likely explanation for its continuous impact on the wettability of the electrospun material, even after deacetylation.

Table 3.4 Hydrophobicity/hydrophilicity of electrospun materials based on the contact angle analysis

No	Sample	Hydrophilicity/hydrophobicity	
		Before deacetylation	After deacetylation
1	Pure CA without any additive	hydrophobic	hydrophilic
2	CA + CuSO <sub>4</sub>	hydrophobic	hydrophilic
3	CA + CuO	hydrophobic	hydrophobic
4	CA + CuSO <sub>4</sub> + Ag (1/8 of CuSO <sub>4</sub> mass)	hydrophilic	hydrophilic
5	CA + CuSO <sub>4</sub> + Ag (1/4 of CuSO <sub>4</sub> mass)	hydrophilic	hydrophilic
6	CA + Cu(OH) <sub>2</sub>	hydrophobic	hydrophilic
7	CA + Cu <sub>2</sub> (OH) <sub>2</sub> CO <sub>3</sub>	hydrophobic	hydrophilic
8	CA + thymol	hydrophilic	hydrophilic
9	CA + CuSO <sub>4</sub> + thymol	hydrophobic	hydrophilic

### 3.2.4 FTIR analysis

To increase the hydrophilic properties of cellulose acetate, the method of deacetylation was applied for the electrospun filter materials [87]-[89]. The success of deacetylation was estimated by FTIR analysis. FTIR analysis was performed on the electrospun filter materials before and after deacetylation. For the two electrospun materials containing Ag NPs, only one sample is presented, as their results were similar. The results can be seen in Figure 3.4-3.11 Comparing the FTIR diagrams of cellulose acetate electrospun filter materials before and after deacetylation shows very clear differences between the peaks marked with red arrows as shown in Figure 3.4, confirming the success of deacetylation.

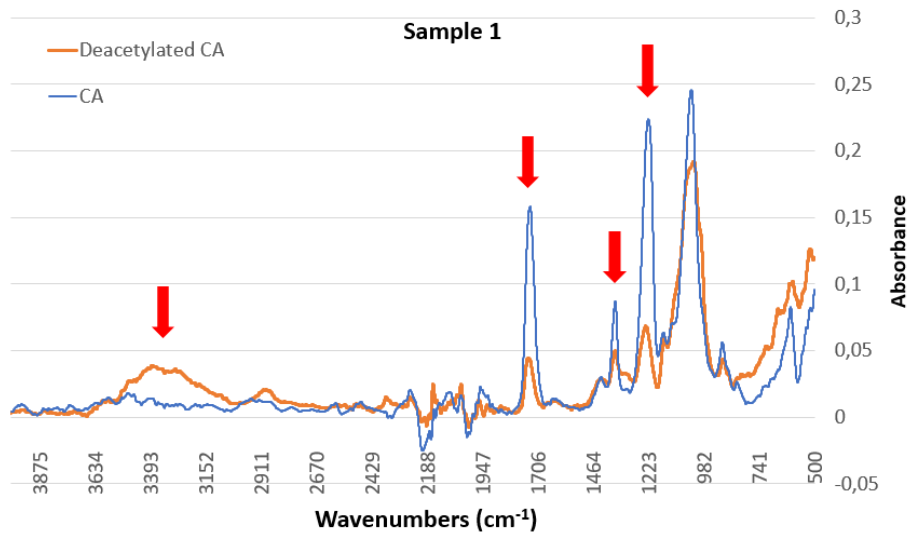


Figure 3.4 FTIR analysis of pure CA material (Sample 1)

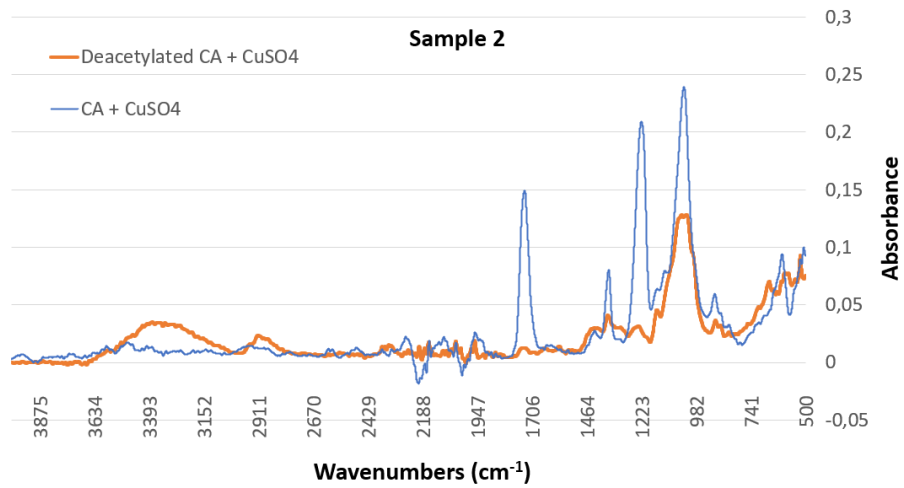


Figure 3.5 FTIR analysis of CA + 18.75% CuSO<sub>4</sub> material (Sample 2)

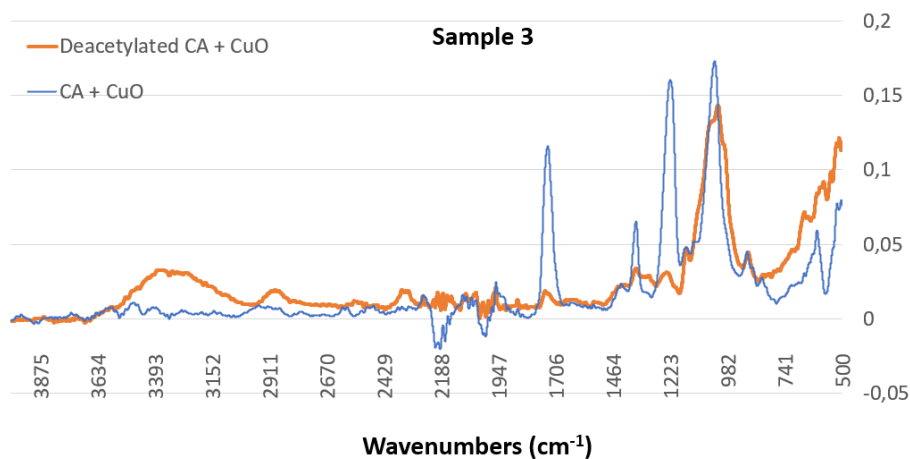


Figure 3.6 FTIR analysis of CA + 12.5% CuO material (Sample 3)

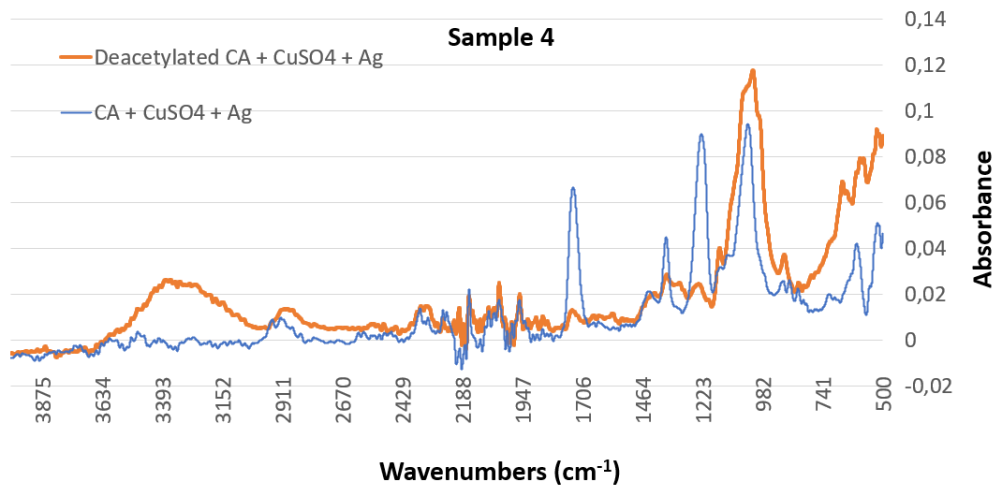


Figure 3.7 FTIR analysis of CA + 18.75% CuSO<sub>4</sub> + Ag (**1/8** of CuSO<sub>4</sub> mass) material (Sample 4)

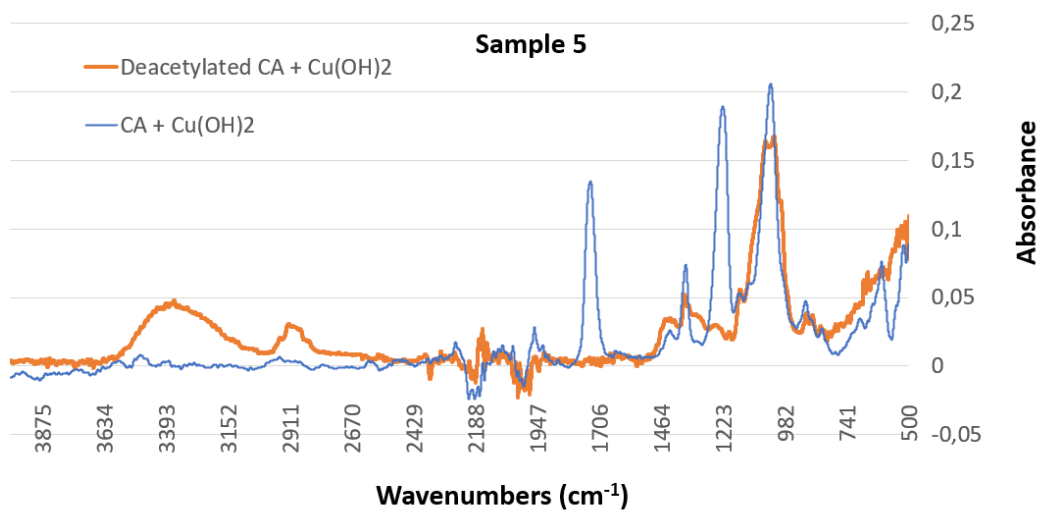


Figure 3.8 FTIR analysis of CA + 9.5% Cu(OH)<sub>2</sub> material (Sample 5)

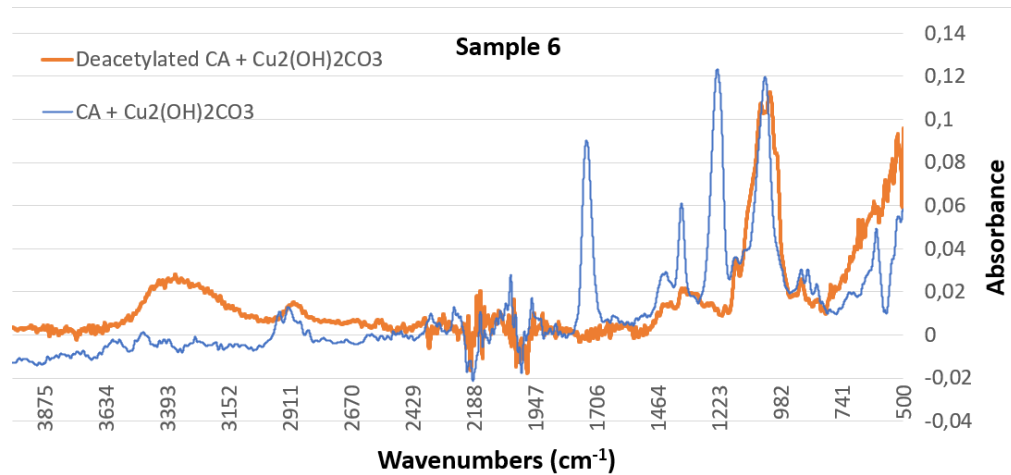


Figure 3.9 FTIR analysis of CA + 14.7% Cu<sub>2</sub>(OH)<sub>2</sub>CO<sub>3</sub> material (Sample 6)



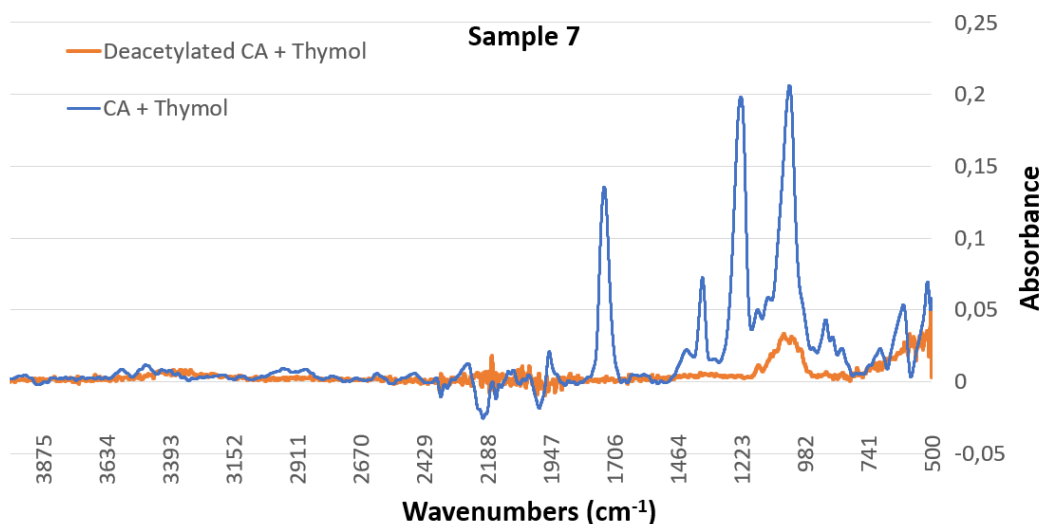


Figure 3.10 FTIR analysis of CA + 10% thymol material (Sample 7)

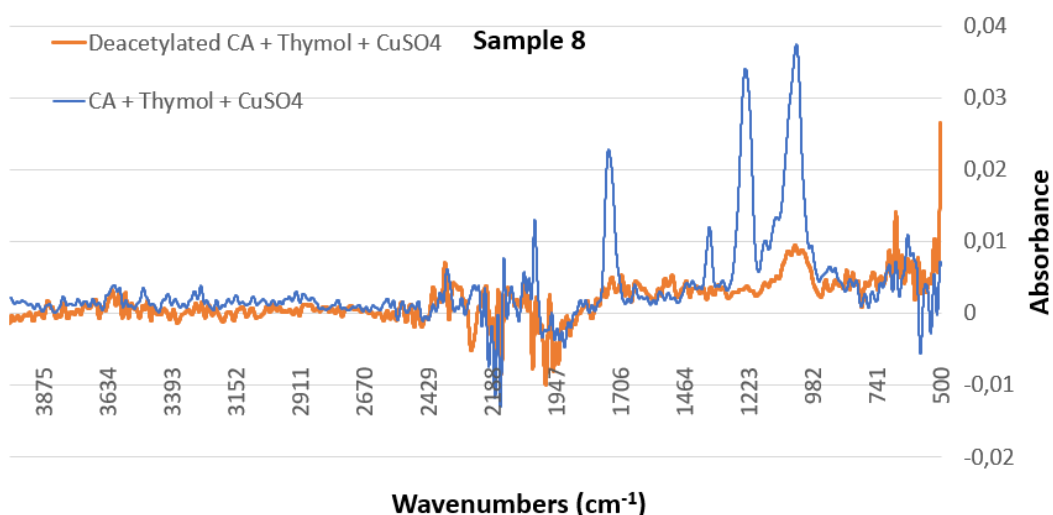


Figure 3.11 FTIR analysis of CA + 10% thymol + 18.75% CuSO<sub>4</sub> material (Sample 8)

For all of the samples, the cellulose acetate curves (blue) have all of the characteristic peaks of cellulose acetate, that were also described in literature, such as peak at 1745  $\text{cm}^{-1}$ , representing C=O bond, the peak representing C-CH<sub>3</sub> bond at 1375  $\text{cm}^{-1}$ , as well as the peak at 1235  $\text{cm}^{-1}$ , which stands for C-O-C bond. As was confirmed by literature, these peaks should disappear if deacetylation is successful and regenerated cellulose is achieved (orange curves), and the acetate group has been removed [88]. The success of deacetylation is confirmed by the disappearance of these peaks.

The diagrams in Figures 3.4-3.9 also confirm the success of deacetylation with the broad and rather flat curve at approximately 3200-3500  $\text{cm}^{-1}$ , which is distinct for the absorbance of the hydroxyl group (-OH), that have successfully replaced the acetate

groups during the deacetylation process [98] [99]. However, for the samples containing thymol in Figures 3.10-3.11, no flat curve at approximately 3200-3500  $\text{cm}^{-1}$  can be seen. It has been noted in literature that hydroxyl groups absorbance in FTIR can have variations based on environmental factors [99]. As all the other characteristic cellulose acetate peaks are not present in the post-deacetylation blue graph in Figures 3.10-3.11 and success of deacetylation is thus confirmed, it can be argued, that addition of thymol might have caused this unexpected phenomenon, as well as the extra noise observed in Figures 3.10-3.11, in the form of small and frequent peaks.

During deacetylation, it was observed that the delicate structure of electrospun filter materials might require a more careful and refined process for deacetylation to be created, in order to produce deacetylated electrospun filter materials. This was especially critical during rinsing of the electrospun filter materials following the deacetylation process, before they were dried. It was also observed, that deacetylation caused the electrospun layer to lose some of its elasticity.

In conclusion, using deacetylation to improve hydrophilic properties of the electrospun filter materials is plausible only if method for rinsing the materials post deacetylation can be made gentler, such as a water bath system with constant and slow water flow perpendicular to the material surface.

### **3.2.5 Measurement of Metal Content of the Materials**

Metal concentration in electrospun filter materials was studied with X-ray analytical instrument S2 PICOFOX. The results can be seen in Table 3.5. Differences between theoretical metal concentration based on the nominal concentration of additive used and measured metal concentration can be explained by various reasons: during electrospinning process, when the needle is stationary the previously well dispersed metal particles could form colloids and sediment to the bottom half of the syringe barrel, thus being a cause of altered actual metal concentration in the polymer fibers. However, the measured Cu concentrations are sufficiently high to improve the antimicrobial properties of the electrospun filter materials, as will be discussed in the following chapters.

Table 3.5 Measured metal particle concentration results in electrospun filter materials

<b>No</b>	<b>Additives</b>	<b>Nominal concentration of pure Cu, %</b>	<b>Measured concentration of Cu, %</b>	<b>Measured concentration of Ag, %</b>
1	-	-	-	-
2	18.75% CuSO <sub>4</sub>	7.5	5.5	-
3	12.5% CuO	10	7.7	-
4	18.75% CuSO <sub>4</sub> + 2.34% Ag ( <b>1/8</b> of CuSO <sub>4</sub> mass)	7.5	5.8	0.2
5	18.75% CuSO <sub>4</sub> + 4.69% Ag ( <b>1/4</b> of CuSO <sub>4</sub> mass)	7.5	2.42	0.003
6	9.5% Cu(OH) <sub>2</sub>	7.5	3.84	-
7	14.7% Cu <sub>2</sub> (OH) <sub>2</sub> CO <sub>3</sub>	7.5	4	-
8	10% thymol	-	-	-
9	18.75% CuSO <sub>4</sub> and 10% thymol	7.5	4.95	-

### 3.2.6 Air Permeability of Electrospun Filter Materials

To characterise the air permeability of the produced filter materials, an air permeability test was used. The air permeability is estimated by measuring differential pressure (ISO 139-2005 and EVS-EN 14683:2019). All electrospun materials including the ones treated by deacetylation process were tested. The results can be seen in Table 3.6 where differential pressure is used as the characteristic of the air permeability of the material. The higher the differential pressure the lower the air permeability of the tested material.

Table 3.6 Air permeability testing of the electrospun filter materials

No	Sample	Differential pressure [Pa/cm <sup>2</sup> ]	
		Before treatment by deacetylation	After treatment by deacetylation
1	Pure CA without any additives	125	125
2	CA + CuSO <sub>4</sub>	<b>54.1</b>	94.5
3	CA + CuO	<b>47.4</b>	31.9
4	CA + CuSO <sub>4</sub> + Ag (1/8 of CuSO <sub>4</sub> mass)	19.7	1.3
5	CA + CuSO <sub>4</sub> + Ag (1/4 of CuSO <sub>4</sub> mass)	16.8	3.9
6	CA + Cu(OH) <sub>2</sub>	-	-
7	CA + Cu <sub>2</sub> (OH) <sub>2</sub> CO <sub>3</sub>	22.7	0.82
8	CA + thymol	<b>45.4</b>	61.9
9	CA + CuSO <sub>4</sub> + thymol	<b>55.9</b>	2.5

Air permeability of the electrospun materials without added metal NPs and compounds does not seem promising to be used for filtering purposes, as differential pressure result of 125 Pa shows that the differential pressure is out of the scope of measurable values for the device. However, the use of additives improves the air permeability of the electrospun materials demonstrating the differential pressure results of 54.1 Pa and 47.4 Pa.

According to literature, optimal differential pressure results for good breathability should remain under 49 Pa [163]. This guideline is met by five electrospun filter materials, as can be seen in Table 3.6. The material containing Cu(OH)<sub>2</sub> (Sample 6) presented inconclusive results due to structural damage to the material during deacetylation and

cannot be compared in this area. Although the breathability levels of some electrospun filter materials exceeded the 49 Pa guideline very slightly, this can refer to the electrospun materials' nonuniformity of thickness along the tested area.

Addition of thymol (Samples no 8-9) to the electrospinning solution reduced air permeability of electrospun materials significantly. When comparing Sample 7 (without thymol) and Samples 8-9 (with thymol), exactly the same amount of solution was used to electrospin these materials. The resulting electrospun materials also had very similar thickness measurement results, ranging between 0.026 mm and 0.029 mm. Yet the air permeability of Sample 8 and Sample 9, containing Thymol, is twice as high as the air permeability for Sample 7.

Electrospun filter materials have a delicate structure [9], which sustained some damage during deacetylation and washing in case of Samples 3-7 and 9, which lowered the air permeability test result values. Unfortunately, these measurements cannot be analysed. Sample 2 and Sample 8 were the only ones, whose structure remained sufficiently uniform, to provide trustworthy measurement results. As can be seen in Table 3.6, deacetylation raised the differential pressure significantly (Sample 2, Sample 8).

If deacetylation is used to improve hydrophilic properties of the samples, the electrospun layer of the filter materials needs to have a very low thickness in order to balance out the decrease in air permeability and breathability, which can be associated with deacetylation. As it has been noted, that electrospun materials have a very delicate structure, it is suggested to develop the deacetylation process further, to make it more gentle for the electrospun filter material.

For the purpose of increasing filtering efficiency of the electrospun material while retaining good breathability, various processes have been suggested in literature. Modifications of the electrospinning material structure to obtain better interfiber porosity can achieve this goal. Corona treated (charged) electrospun material could also have the same effect, as this process creates higher charge densities, promoting a stronger electrostatic mechanism of the filter material, resulting in improved filtering properties. When comparing the same basis weight ( $\text{g/m}^2$ ), improved breathability can also be obtained, if electrospun fiber diameters are adjusted and multi-layer approach is used, meaning that the same basis weight is divided between many layers, which are stacked together, instead of using just one layer with the same basis weight. It has been also noted, that altering the order of the layers in the multi-layer approach can change the breathability of the material. For nanofibrous filter materials, lower basis weight is usually preferred, for high filtration performance and low pressure drop [125], however

some sources do claim, that thicker filter materials are linked to increased filtration efficiency [164].

### 3.2.7 Effectiveness Of Aerosol Particles Filtration

Aerosol particles filtration effectiveness is a highly important characteristic of filter materials, which was estimated according to EVS-EN 13274 and ASTM F2299/F2299M, using polydisperse aerosol with particle range of 11.8-429.4 nm. The 300 nm particle size represents the particle range which N95 masks are certified to filtrate [144]. N95 masks are able to filtrate 95% of particles with diameters as small as 300 nm [165]. The main way of transmission for the SARS-CoV-2 virus particles is considered to be airborne respiratory particles (<5–10  $\mu\text{m}$  diameter) produced by infected subjects [103]. SARS-CoV-2 particle size has been determined to fall in the range of 50-140 nm [117], which is covered by the whole range of aerosol particles filtration effectiveness test. The results of aerosol particles filtration efficiency test can be seen in Table 3.7, which estimates the filtration effectiveness by comparing the aerosol concentration before and after passing through the electrospun materials.

Table 3.7 Aerosol particles filtration test results

No	Sample	Sample thickness, mm	Effectiveness of aerosol particles filtration, %	
			Whole range 11.8-429.4 nm	300 nm
1	Pure CA without any additives	0.051	<b>99.3</b>	<b>99.6</b>
2	CA + CuSO <sub>4</sub>	0.062	<b>84.3</b>	<b>85.5</b>
3	CA + CuO	0.163	78.4	81.6
4	CA + CuSO <sub>4</sub> + Ag (1/8 of CuSO <sub>4</sub> mass)	0.034	65.8	60.4
5	CA + CuSO <sub>4</sub> + Ag (1/4 of CuSO <sub>4</sub> mass)	0.017	66.9	62.4
6	CA + Cu(OH) <sub>2</sub>	0.047	<b>95.5</b>	<b>98.2</b>
7	CA + Cu <sub>2</sub> (OH) <sub>2</sub> CO <sub>3</sub>	0.026	65.3	61.7

The only electrospun materials that exceeded the N95 masks 95% filtration requirement for minimum 300 nm particles were pure CA electrospun material and the CA electrospun material that contained Cu(OH)<sub>2</sub> additive.

Predictably the aerosol particle filtration efficiency is linked with sample thickness, with both of the high filtration efficiency materials having thicknesses ranging between 0.047-0.051 mm. Materials with lowest test results in the aerosol particles filtration efficiency test had thickness values roughly twice as low, ranging between 0.017 (Sample no 5) to 0.034 mm (Sample no 4).

Based on these observations, CA electrospun material that contains  $\text{Cu}(\text{OH})_2$  additive has the best aerosol particle filtration efficiency compared to all the other electrospun materials containing other additives.

### **3.2.8 Antibacterial Properties of Electrospun Filter Materials**

Antibacterial properties of filter materials were studied against bacteria. Bacteria can be divided into two major groups based on the structure of the cell membranes – Gram-negative and Gram-positive [166]. An example of a Gram-negative bacteria is *Escherichia coli* (*E.coli*) whereas *Staphylococcus aureus* (*S.aureus*) belongs to the Gram-positive bacteria category [147], [148]. Pathogenic strains of *E.coli* and *S.aureus* are also the cause of infections in hospitals and are proven to develop resistance against antibiotics [149]. Antibacterial properties against *E.coli* and *S.aureus* were studied by evaluating the growth of these bacteria on the surface of the electrospun filter materials, as can be seen in Table 3.8. Tight growth of bacteria after incubation (C) indicates that the material does not possess antibacterial properties, as tight bacterial growth can be seen on the surface of the sample. For the samples showing no growth (A) or slight growth (B) of bacteria, it can be concluded that these materials have antibacterial properties, inhibiting bacterial growth on these materials [167].

Table 3.8 Visual evaluation of bacteria growth on electrospun filter materials

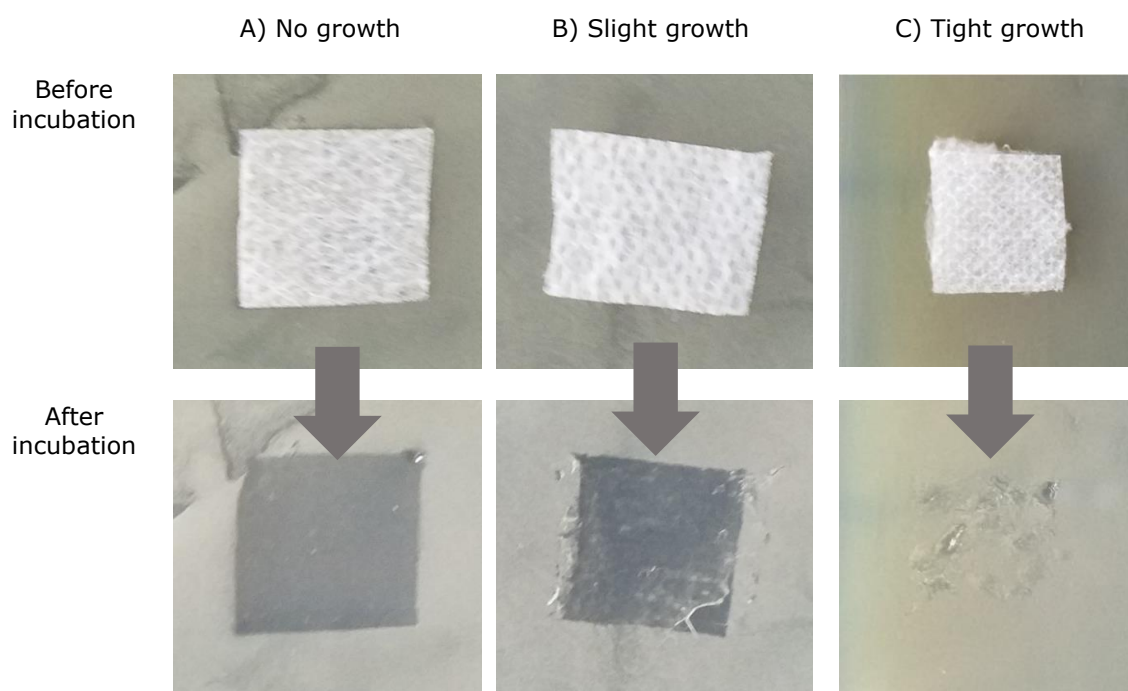


Table 3.9 Electrospun material antibacterial efficiency

No	Name	Antibacterial efficiency against	
		E. coli	S. aureus
2	CA + CuSO <sub>4</sub>	Yes	Yes
3	CA + CuO	Yes	Yes
4	CA + CuSO <sub>4</sub> + Ag (1/8 of CuSO <sub>4</sub> mass)	Yes	Yes
5	CA + CuSO <sub>4</sub> + Ag (1/4 of CuSO <sub>4</sub> mass)	No	Yes
6	CA + Cu(OH) <sub>2</sub>	Yes	No
7	CA + Cu <sub>2</sub> (OH) <sub>2</sub> CO <sub>3</sub>	Yes	Yes
8	CA + thymol	Yes	Yes
9	CA + CuSO <sub>4</sub> + thymol	Yes	Yes

As it can be seen from Table 3.9 the electrospun filter materials with metal additives have shown very promising results in terms of antibacterial efficiency, with only Sample 6 containing Cu(OH)<sub>2</sub> showing tight growth with *S. aureus* and Sample 5 containing CA + CuSO<sub>4</sub> + Ag (1/4 of CuSO<sub>4</sub> mass) showing tight growth with *E. coli*.



It could be argued, that in the case of the Sample 5, CA + CuSO<sub>4</sub> + Ag (1/4 of CuSO<sub>4</sub> mass), the *E. coli* growth sample was cut from an area of the material, where electrospun fibers with antimicrobial additives were not sufficiently high. This is because Sample 4 material containing the same additives with lower concentration of Ag showed antibacterial properties against both *E. coli* and *S. aureus*.

Based on a closer evaluation of each materials' growth with both bacteria, the following compounds had the best antibacterial properties - CuSO<sub>4</sub>, CuO and Cu<sub>2</sub>(OH)<sub>2</sub>CO<sub>3</sub>. As these compounds have excellent antimicrobial properties, it was suggested that electrospun filter materials containing them would also have antiviral properties.

### **3.2.9 Antiviral Properties of Electrospun Filter Materials**

Antiviral properties of electrospun filter materials were evaluated against the SARS-CoV-2 Delta (Indian) isolate using the plaque assay. Three samples of the same dilution were used. Titers illustrating the plaque forming units per millilitre (PFU/ml) were calculated and compared after 5 minutes and 60 minutes. The results can be seen in Figure 3.12. The choice of conducting antiviral tests with the electrospun materials containing CuO and CuSO<sub>4</sub> additives was based on the highest measured Cu concentration in electrospun material determined by measuring and comparing all copper compound additives used in the present study. These antimicrobial additives have also proven activity against many pathogens including MRSA and *E. coli* [70], [71], [74]. The antibacterial tests in this thesis also confirmed this activity. The hypothesis of this thesis is that the antimicrobial additives that have antibacterial efficiency are also effective against viruses such as SARS-CoV-2.

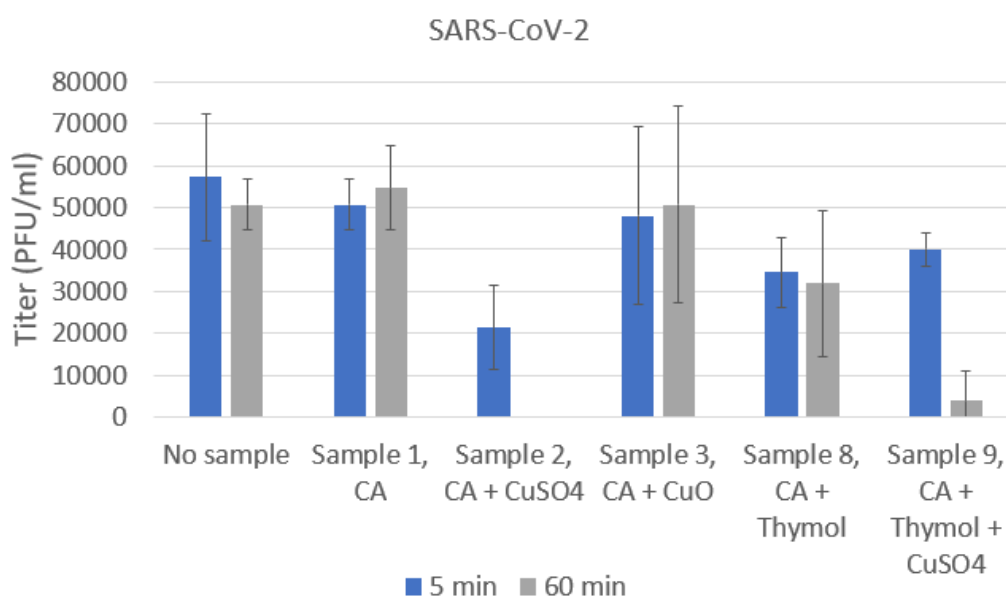


Figure 3.12 Antiviral properties of the selected electrospun filter materials against SARS-CoV-2 Delta (Indian) isolate

Comparison of Sample 1 of pure CA electrospun material to the control (an electrospun material without additives) illustrates that pure CA material does not have any antiviral properties. Also, the addition of CuO NPs does not give the antiviral properties to the CA electrospun material (Figure 3.12 Sample 3 titer calculations).

The addition of CuSO<sub>4</sub> on the other hand gives significant antiviral properties to CA electrospun filter material (Sample 2), showing excellent antiviral properties after only 5 minutes and total elimination of SARS-CoV-2 after 60 minutes. The combination of thymol and CuSO<sub>4</sub> in CA nanofibers (Sample 9) has also good antiviral properties against SARS-CoV-2.

As stated in literature [57]–[59] and confirmed by the antiviral tests in this thesis, using antimicrobial additive thymol increases the antiviral properties of CA electrospun filter material (Sample 8) but is not as efficient as CuSO<sub>4</sub> additive.

## 4. SUMMARY

The aim of the current master's thesis "Electrospun Filter Materials with Enhanced Protective Properties" was to successfully produce electrospun filter material with improved protective properties against viruses like SARS-CoV-2 by the means of electrospinning. RNA viruses like SARS-CoV-2, which caused a global pandemic, are known to mutate into new variants and proved to be unpredictable in terms of resistance to vaccines, rate of spread and severity [2]–[4], thus masks are highly important for preventing the spread of SARS-CoV-2 [2], [5]. The novelty of this thesis is based on using antimicrobial nanoparticle and metal compound additives in electrospinning solution to create nanofibrous filter materials with enhanced protective properties.

To achieve the aim of this thesis, electrospun materials with a variety of additives were produced, followed by a selection of tests and analysis to determine the suitability of these materials to be used as filter materials with enhanced protective properties. Conducted analysis and tests on all filter materials helped to understand different aspects of using copper compound additives in electrospinning and how these affect the electrospinning process and electrospun material properties.

Although the concentration of added metal NPs and metal compounds was very small, its effects on the electrospinning process, fiber structure and other characteristics was notable. The effects of each metal compound additive on the material thickness and air permeability was different and most likely closely linked to the specific metal NPs and metal compounds used. The effect of the metal additive on the electrospinning process for the material production is an important topic, that is essential to be studied further.

Deacetylation process, aiming to improve hydrophilic properties of new electrospun filter materials, was successful, as confirmed by the FTIR results and hydrophilicity estimations. Electrospun filter materials have a delicate structure [9] and some samples were damaged during deacetylation and washing. To use deacetylation on electrospun filter materials, possibilities to develop the deacetylation process further and make it more gentle for the electrospun filter material could be researched.

Based on the cross-examination of analysis results, three electrospun filter materials containing antimicrobial metals had excellent test results, confirming the successful production of electrospun filter materials with antiviral properties. Electrospun material produced from the solution of CA +  $\text{Cu}_2(\text{OH})_2\text{CO}_3$  in acetone-DMAc (2:1) had excellent antibacterial properties against *E.coli* and *S.aureus*, good breathability, suitable fiber

diameters and slightly grooved fiber surface which improves the filtration efficiency of the material.

Electrospun material produced from the solution of CA + **Cu(OH)<sub>2</sub>** in acetone-DMAc (2:1) had excellent aerosol filtration efficiency, antibacterial properties against *E.coli* and suitable fiber diameters with lightly grooved fiber surface which was a contributing factor for achieving best filtration efficiency.

Electrospun material produced from the solution of CA + **CuSO<sub>4</sub>** in acetone-DMAc (2:1) had outstanding antiviral properties against SARS-CoV-2, good aerosol filtration efficiency, excellent surface morphology with grooved fibers and small fiber diameters as well as excellent antibacterial properties against *E.coli* and *S.aureus*. Increased breathability of this material could be studied further, as the differential pressure of this material was slightly over the optimal differential pressure limit proposed by literature for good breathability [163].

The electrospun material containing **CuSO<sub>4</sub>** additive has shown the most promising results to be used as electrospun filter material with enhanced protective properties. However further research is required to determine the best method to achieve increased breathability of this material.

## 5. KOKKUVÕTE

Magistritöö "Parendatud kaitseomadustega elektrokedratud filtermaterjalid" eesmärk oli luua parendatud viiruste vastaste omadustega elektrokedratud filtermaterjal, mis omaks antiviraalset toimet näiteks SARS-CoV-2 vastu. Ülemaailmse pandeemia põhjustajaks olnud SARS-CoV-2 on RNA-viirus, mis muteerub pidevalt ning uute mutatsioonide levik, ohtlikkus ning allumine vaktsiinidele on ettearvamatu [2]–[4]. Seepärast on maskid olulised takistamaks SARS-CoV-2 levikut [2], [5]. Käesoleva magistritöö uudsus seisneb antimikroobsete nanoosakeste ja metalliühendite kasutamises elektroketruse lahuste lisanditena, et luua elektrokedratud filtermaterjale millel on parendatud kaitseomadused.

Magistritöö eesmärgi saavutamiseks loodi elektrokedratud materjalid, mis sisaldavad erinevaid lisandeid. Elektrokedratud materjalidega sooritati erinevaid teste ja analüüse, et tuvastada materjalide omaduste sobilikkus parendatud kaitseomadustega filtermaterjalidena kasutamiseks, mis aitasid saada ülevaadet lisanditena kasutatud metalliühendite mõju kohta elektroketruse protsessile ning elektrokedratud materjalidele.

Kuigi lisandina kasutatud metallist nanoosakeste ja ühendite kontsentratsioon oli väga väike, avaldasid nad suurt mõju elektroketruse protsessile ja kiu struktuurile. Spetsiifilistest lisanditest tingitud variatsioone oli märgata muuhulgas materjali läbilõike paksuse ja õhuläbilaskvuse puhul. Metallühendite poolt avaldatud mõju elektroketruse protsessile ning elektrokedratava materjali omadustele on oluline teema, mida tasub põhjalikumalt uurida tulevikus.

Deatsetüleerimise protsessi eesmärk oli parandada elektrokedratud filtermaterjalide hüdrofiilseid omadusi. Protsessi edu kinnitasid FTIR tulemused ning hüdrofiilsuse mõõtmise tulemused. Elektrokedratud filtermaterjalide õrna struktuuri [9] tõttu said mõned elektrokedratud materjalid deatsetüleerimise protsessi ning sellele järgnenud loputamise käigus kahjustada. Elektrokedratud materjalide deatsetüleerimiseks oleks vaja protsessi arendada ning muuta seda õrnatoimelisemaks.

Sooritatud testide ja analüüside põhjal paistsid oma heade omaduste poolest silma kolm antimikroobseid lisandeid sisaldavat elektrokedratud filtermaterjali, kinnitades parendatud omadustega elektrokedratud filtermaterjalide loomise õnnestumise.

Elektrokedratud materjal mis loodi CA + **Cu<sub>2</sub>(OH)<sub>2</sub>CO<sub>3</sub>** + atsetoon-DMAc (2:1) lahusest, oli antibakteriaalse mõjuga *E.coli* ja *S.aureus* bakterite vastu, hea

hingavusega, väikese kiu läbimõõtudega ning kiu pinnal oli märgata soonelist ja poorest tekstuuri, mis panustas materjali filtreerimise efektiivsusesse.

Elektrokedratud materjal mis loodi CA + **Cu(OH)<sub>2</sub>** + atsetoon-DMAc (2:1) lahusest, näitas häid tulemusi filtreerimise efektiivsuse testis, oli antibakteriaalse mõjuga *E.coli* bakteri vastu, materjali kiud olid väikese läbimõõduga ning kiu pinnal oli märgata soonelist ja poorest tekstuuri, mis aitas kaasa materjali väga heale filtreerimise efektiivsusele.

Elektrokedratud materjal mis loodi CA + **CuSO<sub>4</sub>** + atsetoon-DMAc (2:1) lahuses, oli väga heade antiviraalsete omadustega SARS-CoV-2 viiruse vastu ja näitas häid tulemusi filtreerimise efektiivsuse testis, oli sobiva morfoloogiaga ning väikese läbimõõduga kiududega millel oli sooneline ja poorne tekstuur. Materjalil olid ka väga head antibakteriaalsed omadused *E.coli* ja *S.aureus* bakterite vastu. Käesoleva elektrokedratud materjali õhuläbilaskvus vajab parendamist, sest diferentsiaalrõhu mõõt ületas vähesel määral soovituslikku optimaalset näomaskide diferentsiaalrõhu ülemmäära [163].

Elektrokedratud materjal mis sisaldas **CuSO<sub>4</sub>** lisandit oli kõige sobivamate omadustega, et kasutada seda parendatud kaitseomadustega elektrokedratud filtermaterjalina. Edasist põhjalikumad uurimist ja arendust vajab materjali õhuläbilaskvus.

## LIST OF REFERENCES

- [1] S. Comunian, D. Dongo, C. Milani, and P. Palestini, "Air pollution and covid-19: The role of particulate matter in the spread and increase of covid-19's morbidity and mortality," *International Journal of Environmental Research and Public Health*, vol. 17, no. 12. MDPI AG, pp. 1–22, Jun. 01, 2020. doi: 10.3390/ijerph17124487.
- [2] "COVID Variants: What You Should Know | Johns Hopkins Medicine." <https://www.hopkinsmedicine.org/health/conditions-and-diseases/coronavirus/a-new-strain-of-coronavirus-what-you-should-know> (accessed Feb. 01, 2022).
- [3] "Naming the coronavirus disease (COVID-19) and the virus that causes it." [https://www.who.int/emergencies/diseases/novel-coronavirus-2019/technical-guidance/naming-the-coronavirus-disease-\(covid-2019\)-and-the-virus-that-causes-it](https://www.who.int/emergencies/diseases/novel-coronavirus-2019/technical-guidance/naming-the-coronavirus-disease-(covid-2019)-and-the-virus-that-causes-it) (accessed Feb. 06, 2022).
- [4] "SARS-CoV-2 variants of concern and variants under investigation- Technical briefing 34".
- [5] "Masks and Respirators." <https://www.cdc.gov/coronavirus/2019-ncov/prevent-getting-sick/types-of-masks.html> (accessed Feb. 06, 2022).
- [6] S. Sundarrajan, K. L. Tan, S. H. Lim, and S. Ramakrishna, "Electrospun nanofibers for air filtration applications," in *Procedia Engineering*, 2014, vol. 75, pp. 159–163. doi: 10.1016/j.proeng.2013.11.034.
- [7] M. Zhu *et al.*, "Electrospun Nanofibers Membranes for Effective Air Filtration," *Macromolecular Materials and Engineering*, vol. 302, no. 1. Wiley-VCH Verlag, Jan. 01, 2017. doi: 10.1002/mame.201600353.
- [8] V. v. Kadam, L. Wang, and R. Padhye, "Electrospun nanofiber materials to filter air pollutants – A review," *Journal of Industrial Textiles*, vol. 47, no. 8. SAGE Publications Ltd, pp. 2253–2280, May 01, 2018. doi: 10.1177/1528083716676812.
- [9] D. Lv *et al.*, "Green Electrospun Nanofibers and Their Application in Air Filtration," *Macromolecular Materials and Engineering*, vol. 303, no. 12. Wiley-VCH Verlag, Dec. 01, 2018. doi: 10.1002/mame.201800336.
- [10] S. Zhang *et al.*, "Electrospun nanofibers for air filtration," in *Electrospinning: Nanofabrication and Applications*, Elsevier, 2018, pp. 365–389. doi: 10.1016/B978-0-323-51270-1.00012-1.
- [11] R. E. Neisiany, M. S. Enayati, A. Kazemi-Beydokhti, O. Das, and S. Ramakrishna, "Multilayered Bio-Based Electrospun Membranes: A Potential Porous Media for Filtration Applications," *Frontiers in Materials*, vol. 7, p. 67, Apr. 2020, doi: 10.3389/fmats.2020.00067.
- [12] F. N. H. Karabulut, G. Höfler, N. A. Chand, and G. W. Beckermann, "Electrospun nanofiber filtration media to protect against biological or nonbiological airborne particles," *Polymers (Basel)*, vol. 13, no. 19, Oct. 2021, doi: 10.3390/POLYM13193257/S1.
- [13] N. Ditaranto, F. Basoli, M. Trombetta, N. Cioffi, and A. Rainer, "Electrospun nanomaterials implementing antibacterial inorganic nanophases," *Applied Sciences (Switzerland)*, vol. 8, no. 9. MDPI AG, Sep. 13, 2018. doi: 10.3390/app8091643.
- [14] A. Haider, S. Haider, and I. K. Kang, "A comprehensive review summarizing the effect of electrospinning parameters and potential applications of nanofibers in biomedical and biotechnology," *Arabian Journal of Chemistry*, vol. 11, no. 8. Elsevier B.V., pp. 1165–1188, Dec. 01, 2018. doi: 10.1016/j.arabjc.2015.11.015.
- [15] J. Matulevicius, L. Kliucininkas, D. Martuzevicius, E. Krugly, M. Tichonovas, and J. Baltrusaitis, "Design and characterization of electrospun polyamide nanofiber media for air filtration applications," *Journal of Nanomaterials*, vol. 2014, 2014, doi: 10.1155/2014/859656.

- [16] L. H. C. X, L. W, W. J, X. Y, and G. Y, "Application of Electrospinning in Antibacterial Field," *Nanomaterials (Basel)*, vol. 11, no. 7, Jul. 2021, doi: 10.3390/NANO11071822.
- [17] W. K. Son, J. H. Youk, and W. H. Park, "Antimicrobial cellulose acetate nanofibers containing silver nanoparticles," *Carbohydrate Polymers*, vol. 65, no. 4, pp. 430–434, Sep. 2006, doi: 10.1016/j.carbpol.2006.01.037.
- [18] W. K. Son, J. H. Youk, T. S. Lee, and W. H. Park, "Electrospinning of ultrafine cellulose acetate fibers: Studies of a new solvent system and deacetylation of ultrafine cellulose acetate fibers," *Journal of Polymer Science Part B: Polymer Physics*, vol. 42, no. 1, pp. 5–11, Jan. 2004, doi: 10.1002/polb.10668.
- [19] H. il Ryu, M. S. Koo, S. Kim, S. Kim, Y. A. Park, and S. M. Park, "Uniform-thickness electrospun nanofiber mat production system based on real-time thickness measurement," *Scientific Reports*, vol. 10, no. 1, Dec. 2020, doi: 10.1038/s41598-020-77985-0.
- [20] A. R. Unnithan, R. S. Arathyram, and C. S. Kim, "Electrospinning of Polymers for Tissue Engineering," *Nanotechnology Applications for Tissue Engineering*, pp. 45–55, Jan. 2015, doi: 10.1016/B978-0-323-32889-0.00003-0.
- [21] O. Hardick, B. Stevens, and D. G. Bracewell, "Nanofiber fabrication in a temperature and humidity controlled environment for improved fiber consistency CORE Metadata, citation and similar papers at core.ac.uk Provided by Nature Precedings".
- [22] N. Angel, L. Guo, F. Yan, H. Wang, and L. Kong, "Effect of processing parameters on the electrospinning of cellulose acetate studied by response surface methodology," *Journal of Agriculture and Food Research*, vol. 2, p. 100015, Dec. 2020, doi: 10.1016/J.JAFR.2019.100015.
- [23] S. Torres-Giner, "Electrospun nanofibers for food packaging applications," *Multifunctional and Nanoreinforced Polymers for Food Packaging*, pp. 108–125, Jan. 2011, doi: 10.1533/9780857092786.1.108.
- [24] Y. Wang, T. Yokota, and T. Someya, "Electrospun nanofiber-based soft electronics," *NPG Asia Materials 2021 13:1*, vol. 13, no. 1, pp. 1–22, Mar. 2021, doi: 10.1038/s41427-020-00267-8.
- [25] "How Surgical Masks are Made, Tested and Used." <https://www.thomasnet.com/articles/other/how-surgical-masks-are-made/> (accessed Feb. 11, 2022).
- [26] R. M. D. Soares, N. M. Siqueira, M. P. Prabhakaram, and S. Ramakrishna, "Electrospinning and electrospray of bio-based and natural polymers for biomaterials development," *Materials Science and Engineering: C*, vol. 92, pp. 969–982, Nov. 2018, doi: 10.1016/J.MSEC.2018.08.004.
- [27] N. Abas, A. Kalair, and N. Khan, "Review of fossil fuels and future energy technologies," *Futures*, vol. 69, pp. 31–49, May 2015, doi: 10.1016/J.FUTURES.2015.03.003.
- [28] S. A. Miller, "Sustainable polymers: Replacing polymers derived from fossil fuels," *Polymer Chemistry*, vol. 5, no. 9, pp. 3117–3118, May 2014, doi: 10.1039/C4PY90017K.
- [29] F. Ciardelli, M. Bertoldo, S. Bronco, and E. Passaglia, "Polymers from Fossil and Renewable Resources," *Polymers from Fossil and Renewable Resources*, 2019, doi: 10.1007/978-3-319-94434-0.
- [30] J. Speirs, C. McGlade, and R. Slade, "Uncertainty in the availability of natural resources: Fossil fuels, critical metals and biomass," *Energy Policy*, vol. 87, pp. 654–664, Dec. 2015, doi: 10.1016/J.ENPOL.2015.02.031.
- [31] "Bio-based products." [https://ec.europa.eu/growth/sectors/biotechnology/bio-based-products\\_en](https://ec.europa.eu/growth/sectors/biotechnology/bio-based-products_en) (accessed Feb. 11, 2022).
- [32] R. Bhardwaj and A. K. Mohanty, "Advances in the Properties of Polylactides Based Materials: A Review," *Journal of Biobased Materials and Bioenergy*, vol. 1, no. 2, pp. 191–209, May 2008, doi: 10.1166/JBMB.2007.023.
- [33] "Sulzer Chemtech", Accessed: Feb. 11, 2022. [Online]. Available: [www.sulzer.com](http://www.sulzer.com)



- [34] D. Yuan, J. Ding, W. Mou, Y. Wang, and Y. Chen, "Bio-based polylactide/epoxidized natural rubber thermoplastic vulcanizates with a co-continuous phase structure," *Polymer Testing*, vol. 64, pp. 200–206, Dec. 2017, doi: 10.1016/J.POLYMERTESTING.2017.10.011.
- [35] M. Kyulavska, N. Toncheva-Moncheva, and J. Rydz, "Biobased Polyamide Ecomaterials and Their Susceptibility to Biodegradation," *Handbook of Ecomaterials*, vol. 4, pp. 2901–2934, Feb. 2019, doi: 10.1007/978-3-319-68255-6\_126.
- [36] M. Winnacker and B. Rieger, "Biobased Polyamides: Recent Advances in Basic and Applied Research," *Macromolecular Rapid Communications*, vol. 37, no. 17, pp. 1391–1413, Sep. 2016, doi: 10.1002/MARC.201600181.
- [37] M. G. Mazzotta, C. M. Reddy, and C. P. Ward, "Rapid Degradation of Cellulose Diacetate by Marine Microbes," <https://www.who.edu/>, vol. 9, no. 1, pp. 37–41, Jan. 2022, doi: 10.1021/ACS.ESTLETT.1C00843.
- [38] J. Ganster and H. P. Fink, "Cellulose and Cellulose Acetate," *Bio-Based Plastics: Materials and Applications*, pp. 35–62, Jan. 2014, doi: 10.1002/9781118676646.CH3.
- [39] "The environmental toll of disposable masks | MIT News | Massachusetts Institute of Technology." <https://news.mit.edu/2021/covid-masks-environment-0720> (accessed Feb. 11, 2022).
- [40] S. Sangkham, "Face mask and medical waste disposal during the novel COVID-19 pandemic in Asia," *Case Studies in Chemical and Environmental Engineering*, vol. 2, p. 100052, Sep. 2020, doi: 10.1016/J.CSCEE.2020.100052.
- [41] K. Selvaranjan, S. Navaratnam, P. Rajeev, and N. Ravintherakumaran, "Environmental challenges induced by extensive use of face masks during COVID-19: A review and potential solutions," *Environmental Challenges*, vol. 3, p. 100039, Apr. 2021, doi: 10.1016/J.ENVC.2021.100039.
- [42] "COVID-19 in Europe: increased pollution from masks, gloves and other single-use plastics — European Environment Agency." <https://www.eea.europa.eu/highlights/covid19-in-europe-increased-pollution> (accessed Feb. 11, 2022).
- [43] O. O. Fadare, B. Wan, L. H. Guo, and L. Zhao, "Microplastics from consumer plastic food containers: Are we consuming it?," *Chemosphere*, vol. 253, p. 126787, Aug. 2020, doi: 10.1016/J.CHEMOSPHERE.2020.126787.
- [44] O. O. Fadare and E. D. Okoffo, "Covid-19 face masks: A potential source of microplastic fibers in the environment," *Science of The Total Environment*, vol. 737, p. 140279, Oct. 2020, doi: 10.1016/J.SCITOTENV.2020.140279.
- [45] V. S. Naragund and P. K. Panda, "Electrospun nanofiber-based respiratory face masks—a review," *Emergent Materials*, vol. 1, pp. 1–18, Jan. 2022, doi: 10.1007/S42247-022-00350-6/TABLES/6.
- [46] J. Wang *et al.*, "Biodegradable and reusable cellulose-based nanofiber membrane preparation for mask filter by electrospinning," *Membranes (Basel)*, vol. 12, no. 1, p. 23, Jan. 2022, doi: 10.3390/MEMBRANES12010023/S1.
- [47] C. Akduman, "Cellulose acetate and polyvinylidene fluoride nanofiber mats for N95 respirators:," <https://doi.org/10.1177/1528083719858760>, vol. 50, no. 8, pp. 1239–1261, Jun. 2019, doi: 10.1177/1528083719858760.
- [48] D. S. de Almeida *et al.*, "Biodegradable CA/CPB electrospun nanofibers for efficient retention of airborne nanoparticles," *Process Safety and Environmental Protection*, vol. 144, pp. 177–185, Dec. 2020, doi: 10.1016/J.PSEP.2020.07.024.
- [49] "Applications: Copper Compounds - Copper Sulphate." [https://www.copper.org/resources/properties/compounds/copper\\_sulfate01.html](https://www.copper.org/resources/properties/compounds/copper_sulfate01.html) (accessed Mar. 29, 2021).
- [50] S. Agarwal, J. H. Wendorff, and A. Greiner, "Use of electrospinning technique for biomedical applications," *Polymer (Guildf)*, vol. 49, no. 26, pp. 5603–5621, Dec. 2008, doi: 10.1016/J.POLYMER.2008.09.014.

- [51] "ElectroSpinning and NanoFibers."  
<https://www.azonano.com/article.aspx?ArticleID=4377> (accessed Apr. 10, 2022).
- [52] J. M. Cornejo Bravo, L. J. Villarreal Gómez, and A. Serrano Medina, "Electrospinning for Drug Delivery Systems: Drug Incorporation Techniques," *Electrospinning - Material, Techniques, and Biomedical Applications*, Dec. 2016, doi: 10.5772/65939.
- [53] R. K. Mishra *et al.*, "Electrospinning production of nanofibrous membranes," *Environmental Chemistry Letters*, vol. 17, no. 2, pp. 767–800, Jun. 2019, doi: 10.1007/S10311-018-00838-W.
- [54] "Thymol | C10H14O - PubChem."  
<https://pubchem.ncbi.nlm.nih.gov/compound/Thymol> (accessed Feb. 11, 2022).
- [55] M. F. Nagoor Meeran, H. Javed, H. al Taei, S. Azimullah, and S. K. Ojha, "Pharmacological properties and molecular mechanisms of thymol: Prospects for its therapeutic potential and pharmaceutical development," *Frontiers in Pharmacology*, vol. 8, no. JUN, p. 380, 2017, doi: 10.3389/FPHAR.2017.00380/BIBTEX.
- [56] "Natural Products," *Pharmacochemistry Library*, vol. 25, no. C, pp. 71–123, Jan. 1997, doi: 10.1016/S0165-7208(97)80025-6.
- [57] Y. Chen, Y. Qiu, W. Chen, and Q. Wei, "Electrospun thymol-loaded porous cellulose acetate fibers with potential biomedical applications," *Materials Science and Engineering C*, vol. 109, Apr. 2020, doi: 10.1016/J.MSEC.2019.110536.
- [58] C. Darpentigny *et al.*, "Antimicrobial Cellulose Nanofibril Porous Materials Obtained by Supercritical Impregnation of Thymol," *ACS Applied Bio Materials*, vol. 3, no. 5, pp. 2965–2975, May 2020, doi: 10.1021/ACSABM.0C00033/SUPPL\_FILE/MT0C00033\_SI\_001.PDF.
- [59] P. Mollarafie, P. Khadiv Parsi, R. Zarghami, M. Amini Fazl, and R. Ghafarzadegan, "Antibacterial and Wound Healing Properties of Thymol (Thymus vulgaris Oil) and its Application in a Novel Wound Dressing," *Journal of Medicinal Plants*, vol. 14, no. 53, pp. 69–81, 2015, Accessed: Feb. 17, 2022. [Online]. Available: <http://jmp.ir/article-1-970-en.html>
- [60] "How Porous Nanofibers Have Enhanced the Engineering of Advanced Materials: A Review | Request PDF", Accessed: Mar. 07, 2022. [Online]. Available: [https://www.researchgate.net/publication/327837554\\_How\\_Porous\\_Nanofibers\\_Have\\_Enhanced\\_the\\_Engineering\\_of\\_Advanced\\_Materials\\_A\\_Review](https://www.researchgate.net/publication/327837554_How_Porous_Nanofibers_Have_Enhanced_the_Engineering_of_Advanced_Materials_A_Review)
- [61] T. Blachowicz and A. Ehrmann, "Most recent developments in electrospun magnetic nanofibers: A review:," <https://doi.org/10.1177/1558925019900843>, vol. 15, pp. 1–14, Feb. 2020, doi: 10.1177/1558925019900843.
- [62] H. Rodríguez-Tobías, G. Morales, and D. Grande, "Comprehensive review on electrospinning techniques as versatile approaches toward antimicrobial biopolymeric composite fibers", doi: 10.1016/j.msec.2019.03.099i.
- [63] S. X. Wang, C. C. Yap, J. He, C. Chen, S. Y. Wong, and X. Li, "Electrospinning: A facile technique for fabricating functional nanofibers for environmental applications," *Nanotechnology Reviews*, vol. 5, no. 1, pp. 51–73, Feb. 2016, doi: 10.1515/NTREV-2015-0065/MACHINEREADABLECITATION/RIS.
- [64] S. Ramakrishna, K. Fujihara, W. E. Teo, T. Yong, Z. Ma, and R. Ramaseshan, "Electrospun nanofibers: solving global issues," *Materials Today*, vol. 9, no. 3, pp. 40–50, Mar. 2006, doi: 10.1016/S1369-7021(06)71389-X.
- [65] X. Zhang, X. Shi, J. E. Gautrot, and T. Peijs, "Nanoengineered electrospun fibers and their biomedical applications: a review," <https://doi.org/10.1080/20550324.2020.1857121>, vol. 7, no. 1, pp. 1–34, 2020, doi: 10.1080/20550324.2020.1857121.
- [66] "Antimicrobial Terminology – microBEnet: the microbiology of the Built Environment network." <https://microbe.net/2014/07/16/antimicrobial-terminology/> (accessed Feb. 18, 2022).

- [67] "Antimicrobial vs Antibacterial - What's the Difference? | Microban." <https://www.microban.com/antimicrobial-solutions/overview/antibacterial-vs-antimicrobial> (accessed Feb. 18, 2022).
- [68] A. A. Cortes and J. M. Zuñiga, "The use of copper to help prevent transmission of SARS-coronavirus and influenza viruses. A general review," *Diagnostic Microbiology and Infectious Disease*, vol. 98, no. 4, p. 115176, Dec. 2020, doi: 10.1016/J.DIAGMICROBIO.2020.115176.
- [69] M. P. Cervantes-Cervantes, J. V. Calderón-Salinas, A. Albores, and J. L. Muñoz-Sánchez, "Copper increases the damage to DNA and proteins caused by reactive oxygen species," *Biological Trace Element Research* 2005 103:3, vol. 103, no. 3, pp. 229–248, Mar. 2005, doi: 10.1385/BTER:103:3:229.
- [70] H. Modarress, A. Eliassi, and E. Keshmirzadeh, "Enthalpy of mixing for polymer solutions based on Gibbs excess function limit of hard spheres mixtures," *Fluid Phase Equilibria*, vol. 235, no. 1, pp. 26–29, Aug. 2005, doi: 10.1016/j.fluid.2005.05.026.
- [71] L. V. Delumeau *et al.*, "Effectiveness of antiviral metal and metal oxide thin-film coatings against human coronavirus 229E," *APL Materials*, vol. 9, no. 11, p. 111114, Nov. 2021, doi: 10.1063/5.0056138.
- [72] S. Behzadinasab, A. Chin, M. Hosseini, L. Poon, and W. A. Ducker, "A Surface Coating that Rapidly Inactivates SARS-CoV-2," *ACS Applied Materials and Interfaces*, vol. 12, no. 31, pp. 34723–34727, Aug. 2020, doi: 10.1021/ACSAMI.0C11425/SUPPL\_FILE/AMOC11425\_SI\_001.PDF.
- [73] V. Govind *et al.*, "Antiviral properties of copper and its alloys to inactivate covid-19 virus: a review," *BioMetals*, vol. 34, no. 6, pp. 1217–1235, Dec. 2021, doi: 10.1007/S10534-021-00339-4/FIGURES/7.
- [74] W. H. de Jong *et al.*, "Toxicity of copper oxide and basic copper carbonate nanoparticles after short-term oral exposure in rats," *Nanotoxicology*, vol. 13, no. 1, pp. 50–72, Jan. 2019, doi: 10.1080/17435390.2018.1530390.
- [75] M. Simonin *et al.*, "Plant and Microbial Responses to Repeated Cu(OH)<sub>2</sub> Nanopesticide Exposures Under Different Fertilization Levels in an Agro-Ecosystem," *Frontiers in Microbiology*, vol. 9, p. 1769, Mar. 2018, doi: 10.3389/FMICB.2018.01769/BIBTEX.
- [76] S. Peixoto, I. Henriques, and S. Loureiro, "Long-term effects of Cu(OH)<sub>2</sub> nanopesticide exposure on soil microbial communities," *Environmental Pollution*, vol. 269, p. 116113, Jan. 2021, doi: 10.1016/J.ENVPOL.2020.116113.
- [77] M. M. Don, C. Y. San, and J. Jeevanandam, "Antimicrobial properties of nanobiomaterials and the mechanism," *Nanobiomaterials in Antimicrobial Therapy: Applications of Nanobiomaterials*, pp. 261–312, Jan. 2016, doi: 10.1016/B978-0-323-42864-4.00008-7.
- [78] T. Mudalige, H. Qu, D. van Haute, S. M. Ansar, A. Paredes, and T. Ingle, "Characterization of Nanomaterials: Tools and Challenges," *Nanomaterials for Food Applications*, pp. 313–353, Jan. 2019, doi: 10.1016/B978-0-12-814130-4.00011-7.
- [79] M. Danaei *et al.*, "Impact of particle size and polydispersity index on the clinical applications of lipidic nanocarrier systems," *Pharmaceutics*, vol. 10, no. 2, pp. 1–17, 2018, doi: 10.3390/pharmaceutics10020057.
- [80] M. S. Ahmed, "Nanofluid: New Fluids by Nanotechnology," *Thermophysical Properties of Complex Materials*, Sep. 2019, doi: 10.5772/INTECHOPEN.86784.
- [81] B. L. Dwornick *et al.*, "Application of Dynamic Light Scattering to Characterize Nanoparticle Agglomeration in Alumina Nanofluids and its Effect on Thermal Conductivity", Accessed: Nov. 01, 2021. [Online]. Available: [http://www.tardec.army.mil,2\\*http://www.swri.org/4org/d08/d08home.htm,3http://www.utsa.edu](http://www.tardec.army.mil,2*http://www.swri.org/4org/d08/d08home.htm,3http://www.utsa.edu)
- [82] K. A. Floyd, A. R. Eberly, and M. Hadjifrangiskou, "Adhesion of bacteria to surfaces and biofilm formation on medical devices," *Biofilms and Implantable Medical Devices: Infection and Control*, pp. 47–95, Jan. 2017, doi: 10.1016/B978-0-08-100382-4.00003-4.

- [83] F. Mikaeili and P. I. Gouma, "Super Water-Repellent Cellulose Acetate Mats," *Scientific Reports* 2018 8:1, vol. 8, no. 1, pp. 1–8, Aug. 2018, doi: 10.1038/s41598-018-30693-2.
- [84] C. D. Zangmeister, J. G. Radney, M. E. Staymates, E. P. Vicenzi, and J. L. Weaver, "Hydration of Hydrophilic Cloth Face Masks Enhances the Filtration of Nanoparticles," *ACS Applied Nano Materials*, vol. 4, no. 3, pp. 2694–2701, Mar. 2021, doi: 10.1021/ACSANM.0C03319/SUPPL\_FILE/AN0C03319\_SI\_001.PDF.
- [85] "Hydrophilic vs Hydrophobic: What's The Difference and How To Select | Medical." <https://www.medical.saint-gobain.com/blog/hydrophilic-vs-hydrophobic-whats-difference-and-how-select> (accessed Nov. 25, 2021).
- [86] "Masks, PPE materials should be hydrophilic -- ScienceDaily." <https://www.sciencedaily.com/releases/2020/08/200811120208.htm> (accessed Nov. 25, 2021).
- [87] T. Budtova and P. Navard, "Cellulose in NaOH-water based solvents: a review Cellulose in NaOH-water based solvents : a review", doi: 10.1007/s10570-015-0779-8i.
- [88] C. Xiang, M. W. Frey, A. G. Taylor, and M. E. Rebovich, "Selective chemical absorbance in electrospun nonwovens," *undefined*, vol. 106, no. 4, pp. 2363–2370, Nov. 2007, doi: 10.1002/APP.26587.
- [89] A. Rezaei, A. Nasirpour, and M. Fathi, "Application of Cellulosic Nanofibers in Food Science Using Electrospinning and Its Potential Risk," *Comprehensive Reviews in Food Science and Food Safety*, vol. 14, no. 3, pp. 269–284, May 2015, doi: 10.1111/1541-4337.12128.
- [90] Y. Zhang, C. Zhang, and Y. Wang, "Recent progress in cellulose-based electrospun nanofibers as multifunctional materials," *Nanoscale Advances*, vol. 3, no. 21, pp. 6040–6047, Oct. 2021, doi: 10.1039/D1NA00508A.
- [91] "Cellulose Acetate." <https://polymerdatabase.com/polymers/Cellulose%20Acetate.html> (accessed Dec. 06, 2021).
- [92] "Cellulose Derivatives." <https://polymerdatabase.com/polymer%20classes/Cellulose%20type.html> (accessed Dec. 06, 2021).
- [93] F. Ahmed *et al.*, "Ultrasonic-assisted deacetylation of cellulose acetate nanofibers: A rapid method to produce cellulose nanofibers," *Ultrasonics Sonochemistry*, vol. 36, pp. 319–325, May 2017, doi: 10.1016/J.ULTSONCH.2016.12.013.
- [94] H. S. Sofi, T. Akram, N. Shabir, R. Vasita, A. H. Jadhav, and F. A. Sheikh, "Regenerated cellulose nanofibers from cellulose acetate: Incorporating hydroxyapatite (HAp) and silver (Ag) nanoparticles (NPs), as a scaffold for tissue engineering applications," *Materials Science and Engineering: C*, vol. 118, p. 111547, Jan. 2021, doi: 10.1016/J.MSEC.2020.111547.
- [95] "FTIR explained in brief | analyticon." <https://www.analyticon.eu/en/ftir.html> (accessed Dec. 06, 2021).
- [96] "How an FTIR Spectrometer Operates - Chemistry LibreTexts." [https://chem.libretexts.org/Bookshelves/Physical\\_and\\_Theoretical\\_Chemistry\\_Textbook/Maps/Supplemental\\_Modules\\_\(Physical\\_and\\_Theoretical\\_Chemistry\)/Spectroscopy/Vibrational\\_Spectroscopy/Infrared\\_Spectroscopy/How\\_an\\_FTIR\\_Spectrometer\\_Operates](https://chem.libretexts.org/Bookshelves/Physical_and_Theoretical_Chemistry_Textbook/Maps/Supplemental_Modules_(Physical_and_Theoretical_Chemistry)/Spectroscopy/Vibrational_Spectroscopy/Infrared_Spectroscopy/How_an_FTIR_Spectrometer_Operates) (accessed Dec. 06, 2021).
- [97] J. Song, N. L. Birbach, and J. P. Hinestroza, "Deposition of silver nanoparticles on cellulosic fibers via stabilization of carboxymethyl groups," *Cellulose*, vol. 19, no. 2, pp. 411–424, Apr. 2012, doi: 10.1007/S10570-011-9647-3.
- [98] "IR Absorption Table." <https://webspectra.chem.ucla.edu/irtable.html> (accessed Dec. 06, 2021).
- [99] "Identifying the Presence of Particular Groups - Chemistry LibreTexts." [https://chem.libretexts.org/Bookshelves/Physical\\_and\\_Theoretical\\_Chemistry\\_Textbook/Maps/Supplemental\\_Modules\\_\(Physical\\_and\\_Theoretical\\_Chemistry\)/S](https://chem.libretexts.org/Bookshelves/Physical_and_Theoretical_Chemistry_Textbook/Maps/Supplemental_Modules_(Physical_and_Theoretical_Chemistry)/S)

- pectroscopy/Vibrational\_Spectroscopy/Infrared\_Spectroscopy/Identifying\_the\_P  
 resence\_of\_Particular\_Groups (accessed Dec. 06, 2021).
- [100] P. C. Raynor and T. M. Peters, "Controlling Nanoparticle Exposures," in *Assessing Nanoparticle Risks to Human Health*, Elsevier, 2016, pp. 153–177. doi: 10.1016/b978-0-323-35323-6.00007-4.
- [101] M. Pan, J. A. Lednicky, and C. Y. Wu, "Collection, particle sizing and detection of airborne viruses," *Journal of Applied Microbiology*, vol. 127, no. 6. Blackwell Publishing Ltd, pp. 1596–1611, Dec. 01, 2019. doi: 10.1111/jam.14278.
- [102] T. R. Sosnowski, "Inhaled aerosols: Their role in COVID-19 transmission, including biophysical interactions in the lungs," *Current Opinion in Colloid & Interface Science*, vol. 54, p. 101451, Aug. 2021, doi: 10.1016/J.COCIS.2021.101451.
- [103] B. U. Lee, "Minimum Sizes of Respiratory Particles Carrying SARS-CoV-2 and the Possibility of Aerosol Generation," *International Journal of Environmental Research and Public Health*, vol. 17, no. 19, pp. 1–8, Oct. 2020, doi: 10.3390/IJERPH17196960.
- [104] J. Lee *et al.*, "Quantity, Size Distribution, and Characteristics of Cough-generated Aerosol Produced by Patients with an Upper Respiratory Tract Infection," *Aerosol and Air Quality Research*, vol. 19, no. 4, pp. 840–853, Apr. 2019, doi: 10.4209/AAQR.2018.01.0031.
- [105] W. G. Lindsley *et al.*, "Quantity and Size Distribution of Cough-Generated Aerosol Particles Produced by Influenza Patients During and After Illness," *Journal of Occupational and Environmental Hygiene*, vol. 9, no. 7, p. 443, Jul. 2012, doi: 10.1080/15459624.2012.684582.
- [106] M. Ehsanifar, "Airborne aerosols particles and COVID-19 transition," *Environmental Research*, vol. 200, p. 111752, Sep. 2021, doi: 10.1016/J.ENVRES.2021.111752.
- [107] "Indoor Air and Coronavirus (COVID-19) | US EPA." <https://www.epa.gov/coronavirus/indoor-air-and-coronavirus-covid-19> (accessed Mar. 03, 2022).
- [108] A. Tcharkhtchi, N. Abbasnezhad, M. Zarbini Seydani, N. Zirak, S. Farzaneh, and M. Shirinbayan, "An overview of filtration efficiency through the masks: Mechanisms of the aerosols penetration," *Bioactive Materials*, vol. 6, no. 1, pp. 106–122, Jan. 2021, doi: 10.1016/J.BIOACTMAT.2020.08.002.
- [109] "Virus." <https://www.genome.gov/genetics-glossary/Virus> (accessed Feb. 04, 2022).
- [110] "Coronavirus Structure, Vaccine and Therapy Development." <https://www.biophysics.org/blog/coronavirus-structure-vaccine-and-therapy-development> (accessed Feb. 01, 2022).
- [111] "Viruses | What is microbiology? | Microbiology Society." <https://microbiologysociety.org/why-microbiology-matters/what-is-microbiology/viruses.html> (accessed Feb. 04, 2022).
- [112] "What Are Viruses? | Live Science." <https://www.livescience.com/53272-what-is-a-virus.html> (accessed Feb. 04, 2022).
- [113] "lipid | Definition, Structure, Examples, Functions, Types, & Facts | Britannica." <https://www.britannica.com/science/lipid> (accessed May 08, 2022).
- [114] K. A. Adedokun, A. O. Olarinmoye, A. O. Olarinmoye, J. O. Mustapha, and R. T. Kamorudeen, "A close look at the biology of SARS-CoV-2, and the potential influence of weather conditions and seasons on COVID-19 case spread," *Infectious Diseases of Poverty*, vol. 9, no. 1, pp. 1–5, Jun. 2020, doi: 10.1186/S40249-020-00688-1/FIGURES/2.
- [115] L. Shao *et al.*, "The role of airborne particles and environmental considerations in the transmission of SARS-CoV-2," *Geoscience Frontiers*, vol. 12, no. 5, p. 101189, Sep. 2021, doi: 10.1016/J.GSF.2021.101189.
- [116] M. Worobey, "Dissecting the early COVID-19 cases in Wuhan," *Science (1979)*, vol. 374, no. 6572, pp. 1202–1204, Dec. 2021, doi: 10.1126/SCIENCE.ABM4454/SUPPL\_FILE/SCIENCE.ABM4454\_SM.PDF.

- [117] "The Size of SARS-CoV-2 and its Implications." <https://www.news-medical.net/health/The-Size-of-SARS-CoV-2-Compared-to-Other-Things.aspx> (accessed May 01, 2022).
- [118] "Time for a paradigm change: understanding COVID-19 disease using next generation innovative, interdisciplinary methodologies | EU Science Hub." <https://ec.europa.eu/jrc/en/news/time-paradigm-change-understanding-covid-19-disease-using-next-generation-innovative> (accessed Feb. 01, 2022).
- [119] "What You Need to Know About Variants | CDC." <https://www.cdc.gov/coronavirus/2019-ncov/variants/about-variants.html> (accessed Feb. 06, 2022).
- [120] R. E. Neisiany, M. S. Enayati, A. Kazemi-Beydokhti, O. Das, and S. Ramakrishna, "Multilayered Bio-Based Electrospun Membranes: A Potential Porous Media for Filtration Applications," *Frontiers in Materials*, vol. 7. Frontiers Media S.A., Apr. 08, 2020. doi: 10.3389/fmats.2020.00067.
- [121] D. P. F. Bonfim, F. G. S. Cruz, V. G. Guerra, and M. L. Aguiar, "Development of Filter Media by Electrospinning for Air Filtration of Nanoparticles from PET Bottles," *Membranes (Basel)*, vol. 11, no. 4, 2021, doi: 10.3390/MEMBRANES11040293.
- [122] A. Mamun, T. Blachowicz, and L. Sabantina, "Electrospun Nanofiber Mats for Filtering Applications—Technology, Structure and Materials," *Polymers (Basel)*, vol. 13, no. 9, May 2021, doi: 10.3390/POLYM13091368.
- [123] T. Lu *et al.*, "Multistructured Electrospun Nanofibers for Air Filtration: A Review," *ACS Applied Materials and Interfaces*, vol. 13, no. 20, pp. 23293–23313, May 2021, doi: 10.1021/ACSAMI.1C06520/ASSET/IMAGES/LARGE/AM1C06520\_0018.JPEG.
- [124] N. E. Zander, "Hierarchically structured electrospun fibers," *Polymers (Basel)*, vol. 5, no. 1, pp. 19–44, Jan. 2013, doi: 10.3390/polym5010019.
- [125] M. Pardo-Figuerez, A. Chiva-Flor, K. Figueroa-Lopez, C. Prieto, and J. M. Lagaron, "Antimicrobial Nanofiber Based Filters for High Filtration Efficiency Respirators," *Nanomaterials*, vol. 11, no. 4, Apr. 2021, doi: 10.3390/NANO11040900.
- [126] J. Li, W. Wang, R. Jiang, and C. Guo, "Antiviral Electrospun Polymer Composites: Recent Advances and Opportunities for Tackling COVID-19," *Frontiers in Materials*, vol. 8, p. 470, Nov. 2021, doi: 10.3389/FMATS.2021.773205/BIBTEX.
- [127] Y. ; Zhou *et al.*, "Electrospun Nanofiber Membranes for Air Filtration: A Review," *Nanomaterials 2022, Vol. 12, Page 1077*, vol. 12, no. 7, p. 1077, Mar. 2022, doi: 10.3390/NANO12071077.
- [128] "Germs: Bacteria, Viruses, Fungi, and Protozoa (for Parents) - Nemours KidsHealth." <https://kidshealth.org/en/parents/germs.html> (accessed Apr. 10, 2022).
- [129] "Germs: Understand and protect against bacteria, viruses and infections - Mayo Clinic." <https://www.mayoclinic.org/diseases-conditions/infectious-diseases/in-depth/germs/art-20045289> (accessed Apr. 10, 2022).
- [130] "Personal protective equipment: MedlinePlus Medical Encyclopedia." <https://medlineplus.gov/ency/patientinstructions/000447.htm> (accessed Apr. 10, 2022).
- [131] "Personal protective equipment | PHA Infection Control." <https://www.niinfectioncontrolmanual.net/personal-protective-equipment> (accessed Apr. 10, 2022).
- [132] S. Karagoz *et al.*, "Antibacterial, Antiviral, and Self-Cleaning Mats with Sensing Capabilities Based on Electrospun Nanofibers Decorated with ZnO Nanorods and Ag Nanoparticles for Protective Clothing Applications," *ACS Appl Mater Interfaces*, vol. 13, no. 4, pp. 5678–5690, Feb. 2021, doi: 10.1021/ACSAMI.0C15606.
- [133] A. Salam *et al.*, "Electrospun Nanofiber-Based Viroblock/ZnO/PAN Hybrid Antiviral Nanocomposite for Personal Protective Applications," *Nanomaterials*

- 2021, Vol. 11, Page 2208, vol. 11, no. 9, p. 2208, Aug. 2021, doi: 10.3390/NANO11092208.
- [134] "EUROPEAN PATENT SPECIFICATION (54) METHOD OF MANUFACTURING NANOFIBER FILTERING MATERIAL FOR DISPOSABLE/REUSABLE RESPIRATORS HERSTELLUNGSVERFAHREN FÜR NANOFASERFILTERMATERIAL FÜR EINWEG-/MEHRWEG-BEATMUNGSVORRICHTUNGEN PROCÉDÉ DE PRODUCTION DE MATÉRIAU DE FILTRATION À NANOFIBER POUR RESPIRATEURS JETABLES/RÉUTILISABLES (84) Designated Contracting States: AL AT BE BG CH CY CZ DE DK EE ES FI FR GB GR HR HU IE IS IT LI LT LU LV MC MK MT NL NO PL PT RO RS SE SI SK SM TR."
- [135] D. Noreña-Caro and M. Alvarez-Láinez, "Experimental design as a tool for the manufacturing of filtering media based on electrospun polyacrylonitrile/  $\beta$  - cyclodextrin fibers," *International Journal on Interactive Design and Manufacturing*, vol. 10, no. 2, pp. 153–164, May 2016, doi: 10.1007/s12008-014-0241-4.
- [136] L. CLEATECH, "Difference Between a HEPA and ULPA Filter | HEPA vs ULPA Filter." <https://www.laboratory-supply.net/blog/difference-between-a-hepa-and-ulpa-filter/> (accessed Mar. 13, 2021).
- [137] "Electrospinning of Nanofibrous Composites with Cellulose Acetate, Ionic Liquids and Graphene Oxide - TalTech raamatukogu digikogu." <https://digikogu.taltech.ee/et/item/e5a1df0c-6583-4141-899d-cbbc95ab4497> (accessed Apr. 25, 2022).
- [138] S. de Vrieze, T. van Camp, A. Nelvig, B. Hagström, P. Westbroek, and K. de Clerck, "The effect of temperature and humidity on electrospinning," *Journal of Materials Science*, vol. 44, no. 5, pp. 1357–1362, Mar. 2009, doi: 10.1007/S10853-008-3010-6.
- [139] Y. Yang, A. Oztekin, S. Neti, and S. Mohapatra, "Particle agglomeration and properties of nanofluids," *Journal of Nanoparticle Research*, vol. 14, no. 5, May 2012, doi: 10.1007/S11051-012-0852-2.
- [140] W. Jeżewski, "Kinetics of aggregation in liquids with dispersed nanoparticles," *Physical Chemistry Chemical Physics*, vol. 17, no. 14, pp. 8828–8835, Mar. 2015, doi: 10.1039/C4CP05401F.
- [141] E. Farrell and J.-L. Brousseau, "Guide for DLS sample preparation".
- [142] "EVS-EN 14683:2019 - Eesti Standardimis- ja Akrediteerimiskeskus." <https://www.evs.ee/et/evs-en-14683-2019> (accessed Mar. 30, 2021).
- [143] "ISO 139:2005 - Eesti Standardimis- ja Akrediteerimiskeskus." <https://www.evs.ee/et/iso-139-2005> (accessed May 07, 2022).
- [144] "What size particle is important to transmission of COVID-19? | Aerosol Laboratory." <https://www.aerosol.mech.ubc.ca/what-size-particle-is-important-to-transmission/> (accessed May 01, 2022).
- [145] "7 ways to measure contact angle." <https://www.biolinscientific.com/blog/7-ways-to-measure-contact-angle> (accessed May 07, 2022).
- [146] K. C. Mills, "Measurement and estimation of physical properties of metals at high temperatures," *Fundamentals of Metallurgy*, pp. 109–177, Jan. 2005, doi: 10.1533/9781845690946.1.109.
- [147] J. Y. Park and K. S. Seo, "Staphylococcus Aureus," *Food Microbiology: Fundamentals and Frontiers*, pp. 555–584, Feb. 2022, doi: 10.1128/9781555819972.ch21.
- [148] J. Y. Lim, J. W. Yoon, and C. J. Hovde, "A Brief Overview of Escherichia coli O157:H7 and Its Plasmid O157," *J Microbiol Biotechnol*, vol. 20, no. 1, p. 5, 2010, doi: 10.4014/jmb.0908.08007.
- [149] A. L. Kubo *et al.*, "Antimicrobial potency of differently coated 10 and 50 nm silver nanoparticles against clinically relevant bacteria Escherichia coli and Staphylococcus aureus," *Colloids and Surfaces B: Biointerfaces*, vol. 170, pp. 401–410, Oct. 2018, doi: 10.1016/J.COLSURFB.2018.06.027.
- [150] J. A. Herrera, J. O. Grande, V. P. Migo, R. E. Arocena, R. D. Manalo, and P. Journal, "Fabrication and Characterization of Electrospun Copper Oxide-Cellulose

- Acetate Microfiber Composite," *Science* (1979), vol. 150, no. 5, pp. 939–950, 2021.
- [151] M. N. Sarwar *et al.*, "Electrospun PVA/CuONPs/Bitter Gourd Nanofibers with Improved Cytocompatibility and Antibacterial Properties: Application as Antibacterial Wound Dressing," *Polymers (Basel)*, vol. 14, no. 7, p. 1361, Mar. 2022, doi: 10.3390/POLYM14071361.
- [152] W. K. Essa, S. A. Yasin, I. A. Saeed, and G. A. M. Ali, "Nanofiber-Based Face Masks and Respirators as COVID-19 Protection: A Review," *Membranes (Basel)*, vol. 11, no. 4, p. 250, Mar. 2021, doi: 10.3390/membranes11040250.
- [153] D. Das, S. Das, and S. M. Ishtiaque, "Optimal design of nonwoven air filter media: Effect of fiber shape," *Fibers and Polymers*, vol. 15, no. 7, pp. 1456–1461, 2014, doi: 10.1007/S12221-014-1456-5.
- [154] E. Vaughn and G. Ramachandran, "Fiberglass Vs. Synthetic Air Filtration Media," *International Nonwovens Journal*, vol. os-11, no. 3, pp. 1558925002OS–01, Sep. 2002, doi: 10.1177/1558925002OS-01100309.
- [155] K. Kuroda, G. A. Caputo, and W. F. DeGrado, "The role of hydrophobicity in the antimicrobial and hemolytic activities of polymethacrylate derivatives," *Chemistry*, vol. 15, no. 5, pp. 1123–1133, Jan. 2009, doi: 10.1002/CHEM.200801523.
- [156] P. Pham, S. Oliver, E. H. H. Wong, and C. Boyer, "Effect of hydrophilic groups on the bioactivity of antimicrobial polymers," *Polymer Chemistry*, vol. 12, no. 39, pp. 5689–5703, Oct. 2021, doi: 10.1039/D1PY01075A.
- [157] B. W. Chieng, N. A. Ibrahim, N. A. Daud, and Z. A. Talib, "Functionalization of Graphene Oxide via Gamma-Ray Irradiation for Hydrophobic Materials," *Synthesis, Technology and Applications of Carbon Nanomaterials*, pp. 177–203, Jan. 2019, doi: 10.1016/B978-0-12-815757-2.00008-5.
- [158] "Explained: Hydrophobic and hydrophilic | MIT News | Massachusetts Institute of Technology." <https://news.mit.edu/2013/hydrophobic-and-hydrophilic-explained-0716> (accessed May 09, 2022).
- [159] "Hydrophilic Silver Coatings | Hydrophilic Treatments for Silver." <https://www.aculon.com/hydrophilic-silver/> (accessed May 09, 2022).
- [160] H. N. H. Veras, F. F. G. Rodrigues, M. A. Botelho, I. R. A. Menezes, H. D. M. Coutinho, and J. G. M. da Costa, "Antimicrobial effect of lippia sidoides and thymol on enterococcus faecalis biofilm of the bacterium isolated from root canals," *The Scientific World Journal*, vol. 2014, 2014, doi: 10.1155/2014/471580.
- [161] Y. He *et al.*, "Hydrophobic CuO Nanosheets Functionalized with Organic Adsorbates," *J Am Chem Soc*, vol. 140, no. 5, pp. 1824–1833, Feb. 2018, doi: 10.1021/JACS.7B11654/SUPPL\_FILE/JA7B11654\_SI\_001.PDF.
- [162] X. Liu, Z. Jiang, J. Li, Z. Zhang, and L. Ren, "Super-hydrophobic property of nano-sized cupric oxide films," *Surface and Coatings Technology*, vol. 204, no. 20, pp. 3200–3204, Jul. 2010, doi: 10.1016/J.SURFCOAT.2010.03.012.
- [163] "Cloth Mask Breathability and Filtration Efficiency Technical Report 1. Executive Summary".
- [164] H. Wang *et al.*, "Development of Electrospun Nanofibrous Filters for Controlling Coronavirus Aerosols," *medRxiv*, p. 2020.12.30.20249046, Jan. 2021, doi: 10.1101/2020.12.30.20249046.
- [165] T. U. Rashid, S. Sharmeen, and S. Biswas, "Effectiveness of N95 Masks against SARS-CoV-2: Performance Efficiency, Concerns, and Future Directions," *Journal of Chemical Health & Safety*, vol. 29, no. 2, pp. 135–164, Mar. 2022, doi: 10.1021/ACS.CHAS.1C00016.
- [166] T. J. Silhavy, D. Kahne, and S. Walker, "The Bacterial Cell Envelope," *Cold Spring Harbor Perspectives in Biology*, vol. 2, no. 5, 2010, doi: 10.1101/CSHPERSPECT.A000414.
- [167] C. Dwivedi *et al.*, "Electrospun Nanofibrous Scaffold as a Potential Carrier of Antimicrobial Therapeutics for Diabetic Wound Healing and Tissue Regeneration," *Nano- and Microscale Drug Delivery Systems: Design and*



*Fabrication*, pp. 147–164, Jan. 2017, doi: 10.1016/B978-0-323-52727-9.00009-1.